T-AM-Sym1 DNA STRUCTURE AND DRUG BINDING STUDIED BY NMR

David E. Wemmer[+], A. Steven Benight[*] and Rachel E. Klevit[*]
+Dept. of Chemistry, University of California, Berkeley, CA 94720
*Dept. of Chemistry, University of Washington, Seattle, WA 98195

The improved resolution and sensitivity of NMR afforded by high field and two-dimensional methods, together with improved methods for oligonucleotide synthesis, have made NMR a powerful approach for examining DNA structures in solution. It is now possible to determine in detail sequence dependent structural effects, interconversion among different structures and binding of various molecules to DNA. Using specifically chosen sequences, we have begun NMR studies of "sticky end" association of oligonucleotides in solution. By measuring imino proton exchange, chemical shifts and linewidths of nonexchangeable protons we can evaluate the equilibrium and kinetic characteristics of association. Using 2DNMR we have investigated the structure of the DNA with particular attention to the region near the gaps in the backbone. The "sticky end" dimers have also been ligated to give single strand circles of DNA, with a central duplex. The melting of these circles has been followed using UV absorption and NMR, and compared to ordinary duplexes of the same sequence. Additional studies have used 2DNMR to characterize the complex of distamycin-A with a DNA dodecamer. From NOEs between the drug and DNA protons, we have determined the binding site of the drug, some effects of binding on the DNA structure, and the dynamics of exchange of drug between DNA molecules.

T-AM-Sym2 EXPLORING MACROMOLECULES BY NUCLEAR SPINS

R.R. Ernst, G. Bodenhausen, M.H. Levitt, N. Müller, C. Radloff, O.W. Sørensen, G. Wagner and K. Wüthrich

Laboratorium für Physikalische Chemie and Institut für Molekularbiologie und Biophysik, Eidgenössische Technische Hochschule, 8092 Zürich, Switzerland

The potential of advanced NMR techniques for the elucidation of molecular structure is discussed. It is demonstrated that the numerous variants of two-dimensional spectroscopy can well be adapted to the experimental situation and provide unique information on molecular structure in solution. A survey is presented on the available techniques for manipulating nuclear spins in view of optimized extraction of the available information.

T-AM-Sym3 HIGH RESOLUTION SOLID-STATE NMR STUDIES OF BACTERIORHODOPSIN

G.S. Harbison[1], S.O. Smith[2,4], D.P. Raleigh[2], J.E. Roberts[2], J.A. Pardoen[3], S.K. Das Gupta[2], J. Lugtenburg[3], R.A. Mathies[4], J. Herzfeld[1], and R.G. Griffin[2]. [1]Harvard Medical School, [2]Massachusetts Institute of Technology, [3]Leiden University, The Netherlands, and [4]University of California, Berkeley.

High resolution solid-state NMR techniques permit studies of a large number of biological systems not accessible with conventional solution methods. Typical of these systems are membrane proteins such as bacteriorhodopsin (bR). Accordingly, we have ^{13}C- and ^{15}N-labeled bR and have examined its magic angle sample spinning (MASS) NMR spectra. The isotropic and anisotropic chemical shifts obtained from these spectra have permitted a determination of a number of features of the retinal chromophore in bR; specifically, the configuration about the C13-C14 and C15-N double and the C6-C7 single bonds and the protonation state of the Schiff base. Evidence is also presented for a negative charge near C-5 and a positive charge near C-7. These results lead to a new model for the retinal binding site in bR and to new implications for the mechanism for the "opsin shift". ^{13}C spectra of specifically ^{13}C-labeled amino acid sidechains -- i.e. tyrosine -- can be used to investigate the putative hydrogen-bonded chain in bR. Spectra of 4-$^{13}C_1$-Tyr are consistent with all of the Tyr's in dark-adapted bR being protonated.

T-AM-Sym4 TWO DIMENSIONAL ^{1}H NMR OF THE CYTOCHROMES C. A.J. WAND
Institute for Cancer Research, Philadelphia, PA 19111

Two dimensional ^{1}H NMR techniques have been applied to the resonance assignment of cytochromes c from several species. The approach used and the current state of the assignment will be summarized. Particular emphasis will be given to problems introduced by the size and spectral complexity of these proteins. Comparison of the J-correlated spectra of six ferrocytochromes has yielded a sufficient library of spin systems assignments to allow a proper sequential assignment to be undertaken. For a number of reasons, the COSY spectra of these proteins fail to consistently yield the complete J-correlated patterns expected of amino acid spin systems. In addition, the COSY spectra are ill-resolved in much of the side chain region. To alleviate these difficulties extensive use of the relayed coherence experiment was required to identify and unravel overlapping spin systems. Phase sensitive NOESY spectra were used to align amino acids in the primary sequence. Even at mixing times of up to 140 ms there is no evidence of significant spin diffusion among backbone protons. The NOESY spectra indicate that most of horse ferrocytochrome c is structurally identical to that indicated by X-ray studies of the tuna enzyme. However, some regions are clearly different. For example, a reverse turn at the C-terminus is found in horse ferrocytochrome c. This structure requires the H-bonding of Glu 104 which is absent in tuna cytochrome c. Backbone dynamics, as a function of redox state, are being followed by H-D exchange and suggest regions of the molecule which are energetically involved in setting the redox potential of the heme. These results, along with a detailed description of the arguments leading to the assignment of the N-terminal helix of horse ferrocytochrome c, will be presented.

T-AM-M ION TRANSPORT MECHANISMS IN SALT TASTE TRANSDUCTION. Sheella Mierson, John A. DeSimone, Gerard L. Heck, and Shirley K. DeSimone, Physiology and Biophysics, Medical College of Virginia, Richmond, VA 23298.

The dorsal lingual epithelium has a unique ion transport system which responds to various salts and other gustatory stimuli. In vitro studies of the tissue from dogs and rats have led to fresh insights into the mechanism of salt taste transduction. Hyperosmotic solutions of univalent salts on the luminal side produce an increase in potential difference (PD) or short-circuit current (Isc) and a decrease in transepithelial resistance (R). Under short-circuited conditions the increase in inward current due to hyperosmotic NaCl is due largely to Na influx. Amiloride partially blocks the response due to hyperosmotic NaCl or LiCl with much less effect on that of KCl; in vivo recordings from the rat chorda tympani show partial inhibition by amiloride of the NaCl or LiCl response with no effect on KCl. In spontaneously hypertensive rats the response to hyperosmotic NaCl is less than in Wistar-Kyoto controls, corresponding to increased taste preferences and decreased chorda tympani responses to NaCl seen in the hypertensive strain. Simultaneous in vivo recordings in the rat of transepithelial PD or Isc and of integrated chorda tympani signal indicate that the transepithelial response precedes the neural response. Preliminary data on NaCl indicate that the onset of neural activity coincides with the inward movement of current and that neural adaptation coincides with the slow or second component in the Isc. Measuring the time courses of the transepithelial response and the rate of neural firing will allow more detailed correlations between the tissue electrophysiological responses and those seen in the gustatory nerve. Supported by NSF BNS-8309135, NIH NS13767, and a grant from Virginia Heart Association.

T-AM-Min2 ELECTRICAL PROPERTIES OF THE FROG OLFACTORY EPITHELIUM IN VITRO. Gerard Heck, John A. DeSimone, and Krishna Persaud, Physiology and Biophysics, Medical College of Virginia, Richmond, Virginia 23298

Odorants applied to the olfactory epithelium of a number of animal species elicit complex surface voltage transients in vivo. These transients are generally thought to represent a summation of potentials at the olfactory receptor level. The presence of surface potentials in an epithelium is presumptive evidence for associated transepithelial currents. Our present studies have demonstrated the presence of odor-induced transepithelial currents in the frog olfactory epithelium in vitro using conventional epithelial voltage-clamping techniques. The dorsal olfactory mucosa was dissected from the nasal cavity, mounted in an Ussing-type chamber and bathed symmetrically in amphibian Ringer's solution. The preparation developed a standing transmucosal potential (non-ciliated side electropositive) indicating active ion transport. Mean values of the open-circuit potential, short-circuit current, and resistance were: 3.8 mV, 56 $\mu A/cm^2$, and 73 Ω-cm^2. Voltage-current curves were linear. Stimulation of the ciliated surface with 2-methoxy-3-isobutylpyrazine in Ringer's resulted in a dose-dependent increase in inward positive current. The current excursions ranged from about 0.2 $\mu A/cm^2$ at the lowest concentration to about 3.7 $\mu A/cm^2$ at the highest. These current magnitudes and the resistance in vitro correspond well to the magnitudes of the odor-induced voltages seen in vivo. The current transient consisted of a rapidly rising first component and a slower second component. The diuretic furosemide, a potent blocker of NaCl cotransport in various epithelia, reduced both the standing and the odorant-induced current.

T-AM-Min3 BRETYLIUM TOSYLATE ENHANCES SALT TASTE. Schiffman, Susan S., Simon, Sidney A., Gill, James M., and Beeker, Timothy G., Duke Medical Center, Durham, N.C.

Amiloride-sensitive sodium channels have been shown to mediate some components of taste in both humans and rats. The diuretic amiloride (n-amidino-3,5-diamino-6-chloropyrazine carboxamide) blocks the taste of Na^+ and Li^+ salts as well as sweet taste in humans and reduces electrophysiological gustatory responses to Na^+ and Li^+ salts in rat. Amiloride also blocks the increases in short circuit current across lingual epithelium induced by Na^+, Li^+ and sugars.

Bretylium tosylate, an antifibrillary drug, has recently been shown to open mucosal, amiloride-sensitive sodium channels in frog skin. It therefore seemed logical to determine whether bretylium might amplify the amiloride-sensitive components of taste.

Results of the experiments to be reported show that bretylium does indeed potentiate the taste of Na^+ and Li^+ salts in humans but has no statistically significant effect on K^+ or Ca^{++} salts. Na^+ and Li^+ are precisely those ions that were found earlier to move through amiloride-sensitive channels. Electrophysiological taste responses in rat to bretylium paralleled the human findings. Furthermore, the potentiation of taste induced by bretylium was completely eliminated by amiloride. However, bretylium had no effect on the short circuit current in isolated dog lingual epithelium. Possible reasons for these findings are discussed.

T-AM-Min4 EFFECTS OF GENOTYPE AND DIETARY SODIUM CHLORIDE ON TASTE RESPONSES IN HYPERTENSIVE AND NORMOTENSIVE RATS. Fay Ferrell. Dept. of Nutrition, University of California, Davis, CA 95616.

The peripheral gustatory system exhibits both developmental plasticity and altered responses with dietary changes or physiologic state. Developmental NaCl deprivation or restriction (Bradley et al., 1983; Hill, 1985) reduces taste nerve responses to NaCl, producing flattened response functions to increasing NaCl concentrations. NaCl deprivation (Contreras, 1977) or adrenalectomy (Kosten and Contreras, 1983) diminishes gustatory nerve activity in NaCl in adult rats. The Dahl salt-sensitive (S) rat is genetically predisposed to become hypertensive if fed a high NaCl diet. The Dahl salt-resistant (R) rat remains normotensive fed the same diet. This study was conducted to learn whether genotype differences exist between (S) and (R) in taste receptor sensitivity to NaCl and to determine whether NaCl taste sensitivities of the two strains are affected by high NaCl feeding. Weanling S and R rats were fed diets containing 8.0% NaCl (High salt) or 0.4% NaCl (Control) for four weeks. Then, with continued feeding of the assigned diet, chorda tympani taste nerve responses were recorded to ascending concentrations of 0.01M - 0.5M NaCl. Expressed as reciprocal plots of conc./response vs. conc., data revealed significant genotype differences in y-intercept and diet-related differences in slope. Assuming the validity of a mass action model, the findings imply that S and R differ in association constants for the interaction between NaCl and taste receptor membrane components. Differences in slope indicate a greater maximal response to NaCl in animals of each strain fed high NaCl diet, possibly due to an increased number of receptors or to heightened effectiveness of the NaCl-receptor interaction. Genotype and diet affect salt taste transdcution, which in turn might influence salt intake in hypertension.

T-AM-Min5 CYCLIC NUCLEOTIDE CASCADE IN OLFACTORY TRANSDUCTION.
Doron Lancet, Zehava Chen, Judith Heldman and Umberto Pace. Department of Membrane Research, The Weizmann Institute of Science, Rehovot, Israel.

The mechanism of olfactory transduction has been largely unknown until recently. Now evidence is accumulating suggesting the involvement of cyclic AMP as a second messenger in vertebrate chemosensory neurons (Pace et al, Nature 316:255 (1985)). Isolated sensory dendritic membrane extensions (olfactory cilia, analogous to rod outer segments) are found to contain extremely high levels of adenylate cyclase, which is specifically activated by various odorants in a GTP-dependent manner. The olfactory GTP-binding protein is similar or identical to G_S, the hormonal stimulatory GTP-binding protein, and is also enriched in the sensory cilia. Thus, odorant receptors may function in a way similar to photoreceptors, hormone and neurotransmitter receptors. Our working hypothesis is that olfactory receptor proteins are a family of similar polypeptides with different odorant binding specificities. Members of this family may share properties such as rough molecular weight, glycosylation, transmembrane disposition and interaction with G_S and the cyclase. A prominent receptor candidate is gp95, a major cilia-specific transmembrane glycoprotein (Chen and Lancet, PNAS 81:1859 (1984)). Reconstitution experiments now underway should help to identify the yet undiscovered olfactory receptors. Odorant-induced cyclic AMP synthesis most probably triggers mambrane depolarization and firing of action potentials in the sensory neuron. We show that olfactory cilia contain cyclic AMP dependent protein kinase, which phosphorylates at least one ciliary polypeptide (pp24). Future single channel recordings should show whether protein phosphorylation and/or direct cyclic nucleotide gating are responsible for ion channel modulation.

T-AM-A1 THE STRUCTURE OF MYOSIN HEAVY CHAIN IN VARIOUS SMOOTH MUSCLES
Gabor Huszar and Lynne Vigue. The Uterine Physiology Unit, Department of Obstetrics and Gynecology, Yale University School of Medicine, P.O. Box 3333, New Haven, CT 06510

Toward the demonstration of possible tissue and species differences, we have examined the structure of smooth muscle myosin heavy chain (SMHC) in gizzards of chickens and turkeys, in dog aorta, and in the human tissues of esophagus, stomach, urinary bladder, uterus, and placenta. The comparison of the uterine SMHC's was also extended to pregnant and non-pregnant cows, and to pregnant rabbits. The SMHC's were chromatographically purified in 5.0 M guanidine-HCl, cleaved with CNBr, and the CNBr peptide digests were subjected to two-dimensional isoelectric focusing/SDS acrylamide gradient gel electrophoresis (Huszar et al, J. Biol. Chem. 260:7249, 1985). The two-dimensional gel patterns demonstrated that the gizzard SMHC's are identical. However, there were well distinguishable differences in the distribution of SMHC's peptides in the various human tissues, which suggest that they are tissue specific isozymes. We also detected species differences among the uterine myosins, but the peptide pattern of uterine SMHC's in non-pregnant and pregnant cows were not different. Furthermore, we found no system specific features characteristic for the gastrointestinal (esophagus and stomach) or urogenital (bladder, uterus, and placenta) SMHC's. Turkey gizzard myosin was also subjected to limited digestion by Staphylococcus aureus protease (Ikebe and Hartshorne, Biochemistry 24:2380, 1985), and the major fragments of the rod and of the subfragment-1 were isolated. CNBr digestion and subsequent two-dimensional electrophoresis demonstrated which of the peptides in the gizzard SMHC digest arise from the rod or from the subfragment-1 part of the molecule (Supported by the Muscular Dystrophy Association).

T-AM-A2 A CONFORMATIONAL TRANSITION IN GIZZARD HEAVY MEROMYOSIN INVOLVING THE HEAD-TAIL JUNCTION STUDIED BY RATES OF DIGESTION OF HEAVY AND LIGHT CHAINS BY PAPAIN. Hiroshi Suzuki, Yoshifusa Kondo, Aida D. Carlos and John C. Seidel, Department of Muscle Research, Boston Biomedical Research Institute, Boston, MA 02114.

Gizzard heavy meromyosin (HMM) undergoes a conformational transition - analogous to the 6S-10S transition of myosin - in which the molecules either are flexed, bent at the neck with the heads projecting back towards the tail, or extended, with one or both heads pointing away from the tail (Suzuki et al., 1985, J. Biol. Chem., in press). The present data indicate that Mg-ATP, phosphorylation and ionic strength all affect the rate of papain digestion at the head-tail junction. Mg-ATP produces a 90% inhibition of the overall degradation rate of the heavy chain by papain, k(h), at 0.03 M NaCl but has no effect at 0.5 M. The dependence of k(h) on $S_{20,w}$, as the NaCl concentration is varied, describes two straight lines with negative and positive slopes with and without Mg-ATP, respectively. Mg-ATP has two effects, shifting an equilibrium between the flexed and extended forms and apparently inducing a localized structural change that reduces k(h) only when HMM is in the flexed form. Data for phosphorylated and dephosphorylated HMM lie on the same straight line suggesting that phosphorylation affects digestability primarily by altering the equilibrium between flexed and extended forms. The 20 kDa light chain, L(20), is cleaved at sites 2 and 4 kDa from the N terminus with phosphorylated and dephosphorylated HMM, respectively. Mg-ATP and ionic strength produce almost identical effects on cleavage of L(20) and the heavy chain of dephosphorylated HMM, while cleavage of L(20) of subfragment-1, whose activity is not regulated by phosphorylation, is nearly independent of Mg-ATP and ionic strength.

T-AM-A3 PHOSPHORYLATION-INDEPENDENT ACTIVATION OF SMOOTH MUSCLE ACTOMYOSIN. Michael P. Walsh and Philip K. Ngai, Department of Medical Biochemistry, University of Calgary, Calgary, Alberta, Canada

Smooth muscle myosin can be prepared free of calmodulin and myosin light chain kinase by Ca^{2+}-dependent hydrophobic interaction chromatography followed by calmodulin-Sepharose affinity chromatography. The actin-activated Mg^{2+}-ATPase activity of this column-purified myosin, like non-purified myosin, requires Ca^{2+}, calmodulin-dependent phosphorylation of its two M_r 20,000 light chains. However, unlike non-purified myosin, column-purified myosin undergoes a time-dependent transition to a form which no longer requires phosphorylation for actin-activation of the myosin Mg^{2+}-ATPase. This transition is due to a slow change in conformation of the myosin from a folded (10S) to an extended (6S) form as shown by: measurement of the myosin Mg^{2+}-ATPase and myosin Ca^{2+}-ATPase in the absence of Ca^{2+} at low and high ionic strength, susceptibility to papain digestion, intrinsic tryptophan fluorescence enhancement upon ATP binding and analytical ultracentrifugation (sedimentation velocity). This conformation transition was caused by slow oxidation of the column-purified myosin, in spite of the presence of 0.2 mM dithiothreitol, since it could be prevented by storage under N_2 and reversed by 5 mM dithiothreitol. These observations: (1) enable the preparation of a form of myosin which is independent of phosphorylation for actin-activation of the Mg^{2+}-ATPase; (2) draw attention to the possibility of unexpected alterations in purified myosin which affect its regulatory properties and may lead to erroneous conclusions about the mechanism of regulation of smooth muscle contraction; (3) provide suitable conditions for the long-term storage of fully-active smooth muscle myosin; and (4) lend further support to the notion that the enzymatic activity of smooth muscle myosin is dictated by its conformation. (Supported by MRC Canada and AHFMR).

T-AM-A4 EXCHANGE OF MOLECULES BETWEEN SMOOTH MUSCLE MYOSIN FILAMENTS. Kathleen M. Trybus & Susan Lowey, Rosenstiel Research Center, Brandeis University, Waltham, MA 02254.

Smooth muscle myosin forms small bipolar aggregates ("minifilaments") composed of 12-14 molecules in 5 mM citrate/22 mM tris. Dephosphorylated minifilaments are dissociated to an antiparallel folded 15S dimer in the presence of 1 mM MgATP, but phosphorylated minifilaments remain assembled. The question of whether dephosphorylated myosin could be stabilized in the filamentous form as a result of interactions with neighboring phosphorylated molecules was investigated. Varying ratios of phosphorylated and dephosphorylated myosin were mixed in high salt and subsequently dialyzed versus citrate/tris in order to form minifilaments containing both species. Upon nucleotide addition to the copolymer, dephosphorylated myosin disassembled to the folded conformation, despite the presence of the more stable phosphorylated molecules. To eliminate the possibility that phosphorylated and dephosphorylated myosin formed separate filaments, copolymers were prepared from mixtures of rod and myosin. Sedimentation velocity experiments showed that this copolymer sedimented with mobility intermediate between 13S rod minifilaments and 22S myosin minifilaments. Similarly to the myosin copolymers, myosin in the rod-myosin filaments was dissociated by MgATP. Copolymers could be formed not only by dialyzing monomeric mixtures into citrate/tris, but also by mixing rod and myosin minifilaments. The time course of copolymer formation was followed by pelleting the minifilaments with actin. Greater than 90% of the rod molecules pelleted after a 10 min incubation of myosin and rod minifilaments, indicating that essentially all filaments contained both rod and myosin. Rapid exchange of molecules in and out of the filament could explain why dephosphorylated myosin in a copolymer is not stabilized by adjacent rod or phosphorylated myosin molecules, but can readily assume the folded conformation upon nucleotide addition.

T-AM-A5 PHOTOAFFINITY LABELING OF THE ACTIVE SITE OF SMOOTH MUSCLE MYOSIN. Yoh Okamoto[1], Takamitsu Sekine[1] and Ralph G. Yount[2], Dept. of Biochemistry[1], Juntendo Univ. School of Medicine, Tokyo, Japan and Biochemistry/Biophysics Program and Dept. of Chemistry[2], Washington State Univ., Pullman, WA., 99164-4660.

The active sites of rabbit skeletal and bovine cardiac myosin have been identified after stable trapping of a photoaffinity analog of ADP, N-(4-azido-2-nitrophenyl)-2-aminoethyl diphosphate (NANDP) either by crosslinking of SH_1 and SH_2 or by addition of vanadate. Photolysis of the MgNANDP myosin·SF_1 complexes resulted in exclusive labeling of Trp_{130} of the heavy chain with no labeling of the light chains. The peptide region around Trp_{130} has a hydrophobic and characteristic nature and the sequence appears to be remarkably conserved in various types of myosin [Y. Okamoto and R. Yount, (1985) Proc. Natl. Acad. Sci. USA, 82, 1575 and unpublished data].

These studies were extended to smooth muscle myosin because gizzard myosin is known to undergo large changes in its conformation and enzymatic properties as a function of light chain phosphorylation, the binding of MgATP, or changes in ionic strength. Photolabeling experiments with smooth muscle myosin (chicken gizzard) in which [^{3}H]NANDP is trapped at the active site with vanadate show that both the heavy chain (24%) and the 17 kDa essential light chains (66%) are labeled. These results indicate the ATP binding sites of gizzard myosin are located at the inter-face of both chains and represent the first direct evidence for participation of the essential light chains in the active site of any type of myosin. This research was supported in part by a Research Grant from the Ministry of Education, Science and Culture of Japan to Y. O. and T. S. and by an NIH Grant AM-05195 and by the Muscular Dystrophy Association to R. G. Y.

T-AM-A6 PREPARATION AND PRELIMINARY CHARACTERIZATION OF HEAVY MEROMYOSIN FROM TURKEY INTESTINAL SMOOTH MUSCLE AND INTESTINAL EPITHELIAL BRUSH BORDER MYOSIN. A. Resai Bengur, Kathleen Faust, Estelle V. Harvey and James R. Sellers. NHLBI, Bethesda, Md. 20892

Many details of the phosphorylation-dependent regulation of the actin-activated MgATPase activity of turkey gizzard smooth muscle myosin have been elucidated. Many of the studies responsible for this information have utilized heavy meromyosin (HMM), the two headed subfragment of myosin. We are attempting to prepare HMM from other phosphorylation-dependent myosins in order to determine how generally relevant the mechanisms determined for gizzard myosin are to other smooth and non-muscle myosins. HMM was prepared from the myosin of turkey intestinal epithelial brush border by chymotryptic digestion. The majority of the 20 kDa light chain was intact as determined by SDS gel electrophoresis and could be phosphorylated by myosin light chain kinase. The HMM had a Vmax of about 0.4 s^{-1} and a Km of 3 uM for the actin-activated MgATPase activity. Direct measurement of the binding constant for actin in the presence of ATP gave a Kd of about 5 uM. The actin-activated MgATPase activity of brush border myosin was not greatly diminished by increasing the ionic strength. We also prepared smooth muscle myosin from turkey intestine. Intestinal smooth muscle myosin had virtually identical affinity for both a polyclonal and a monoclonal antibody prepared against turkey gizzard myosin. By contrast, brush border myosin showed some cross reactivity with the polyclonal, but none with the monoclonal antibody. HMM prepared from intestinal smooth muscle myosin also resembles that from gizzard myosin in its SDS gel pattern. The Vmax of the actin-activated MgATPase activity of phosphorylated intestinal smooth muscle HMM is high whereas that of unphosphorylated HMM is low.

T-AM-A7 THE ACTIN-ACTIVATED ATPases OF UNPHOSPHORYLATED AND PHOSPHORYLATED THYMUS MYOSIN HAVE THE SAME MAXIMUM RATE. Paul D. Wagner, Laboratory of Biochemistry, National Cancer Institute, NIH, Bethesda, Maryland 20892.

Phosphorylation of the 20,000 Da light chains, LC20, of vertebrate smooth and nonmuscle myosins is generally thought to be the primary mechanism for regulating the actin-activated ATPase activities of these myosins. The MgATPase activity of calf thymus myosin has been determined as a function of actin concentration. The maximum rate, V_{max} of the actin-activated ATPase of unphosphorylated thymus myosin (5% phosphorylated LC20) was found to be the same as that of the fully phosphorylated myosin. However, LC20 phosphorylation caused a 15-20 fold decrease in K_{app}, the actin concentration required to achieve 1/2 V_{max}. When actin complexed with either skeletal muscle or calf thymus tropomyosin was used, the values for V_{max} were the same as those obtained with F-actin, but the K_{app} of the unphosphorylated myosin was only 3-5 fold greater than that of the phosphorylated myosin. Thus, LC20 phosphorylation regulates the actin-activated ATPase of thymus myosin not by increasing V_{max} but rather by increasing the apparent affinity of this myosin for actin. In contrast, LC20 phosphorylation appears to regulate the actin-activated ATPase of gizzard myosin by causing a large increase in V_{max}. The rather small differences in the K_{app} values of unphosphorylated and phosphorylated thymus myosin suggest that other proteins may be involved in regulating the actin-activated ATPases of vertebrate nonmuscle myosins.

T-AM-A8 DROSOPHILA CYTOPLASMIC MYOSIN. D.P. Kiehart and R. Feghali, Dept. of Cellular and Developmental Biology, Harvard University, Cambridge, MA 02138

Cytoplasmic myosin was purified from three different Drosophila cell lines (Schneider's lines 2 & 3 and Kc) by cell lysis in a low salt sucrose buffer that contains ATP, chromatography on DEAE-cellulose, precipitation with actin in the absence of ATP, and sizing on an A15m agarose column in high salt. Yields are ~100 ug of purified protein per 30 gm of cells. The protein we purify is myosin by six criteria: its heavy chain molecular weight is ~205 kDa as estimated by SDS-PAGE, it has high ATPase activity in K^+-EDTA (~550 nmol/mg.min), it is recognized by two monoclonal antibodies directed against human platelet myosin, it has a long tail and two heads as demonstrated by electron microscopy of platinum shadowed specimens, it forms bipolar filaments with a conspicuous bare zone and it binds actin in an ATP dependent fashion. The cytoplasmic myosin heavy chain is distinguishable from Drosophila muscle myosin heavy chain by one dimensional, V8-protease peptide maps, by two dimensional tryptic or alpha-chymotryptic peptide maps, and by differential binding of an antibody raised against the cytoplasmic isoform. Experiments in collaboration with L.S.B. Goldstein and R. Laymon indicate that the cytoplasmic myosin is the product of a different myosin gene than the muscle myosin heavy chain gene that has been described (1983 Cell 32:23; 1983 Nature 302: 393). Grant support: NIH CA 31460 & GM 33830, and William F. Milton Fund, Harvard University.

T-AM-A9 BRUSH BORDER MYOSIN HEAVY AND LIGHT CHAIN PHOSPHORYLATION BY CALMODULIN-DEPENDENT KINASES. Rieker, J., Swanljung-Collins, H., Montibeller, J., Lamperski, B., and Collins, J.H. (Intr. by K. W. Snowdowne); Dept. of Microbiology, Biochemistry and Molecular Biology, Univ. of Pittsburgh School of Med., Pittsburgh, PA 15261.

The role of the calmodulin-dependent light chain phosphorylation in actomyosin based contractility of vertebrate smooth muscle and non-muscle cells has been extensively studied. Myosin heavy chain phosphorylation has also been found in vivo in several non-muscle tissues, but no mechanism for regulation of this phosphorylation has been reported. We have identified three myosin kinase activities in the chicken intestinal epithelial cell brush border using isolated brush border myosin as substrate. We show here the partial purification of a myosin heavy chain kinase (MHCK) that is completely dependent on Ca^{2+} and calmodulin for activity. MHCK phosphorylates a threonine residue(s) to about 1.4 mol of phosphate/mol of myosin. We have also partially purified a calmodulin-dependent myosin light chain kinase (MLCK) that phosphorylates a serine residue(s) in the 20-kDa light chains. Phosphorylation by MLCK to about 1.7 mol of phosphate/mol of myosin results in the conversion of myosin from a non actin-activatable ATPase to a form activated 25-fold by actin, to a specific activity of about 0.1 μmol/min/mg. A fraction containing MLCK and MHCK stimulates actin-activatable myosin ATPase activity. MHCK (subunit MW ~ 50,000) is apparently autophosphorylated under conditions in which the kinase is active. We have also identified a Ca^{2+}-independent light chain kinase from brush borders that phosphorylates threonine residues and activates myosin ATPase (see accompanying abstract). Supported by NIH and the March of Dimes grants to J.C., NIH Postdoctoral Training Grant to J.R.

T-AM-A10 THE CONFORMATION OF THE ACANTHAMOEBA MYOSIN II HEAD WHEN BOUND TO F-ACTIN REGULATES THE Mg^{2+}-ATPase ACTIVITY OF THE ACTOMYOSIN II COMPLEX. Mark A.L. Atkinson and Edward D. Korn, Laboratory of Cell Biology, NHLBI, National Institutes of Health, Bethesda, MD 20892.

Myosin II from Acanthamoeba castellanii has an actin-activated Mg^{2+}-ATPase activity which is regulated by phosphorylation of three serine residues near the carboxyl terminus of the molecule. We believe that the C-terminal 85 amino acids are essential for both filament formation and actin-activated Mg^{2+}-ATPase activity, and that enzyme activity is exquisitely sensitive to filament conformation. To investigate this hypothesis further, we have generated a single-headed myosin II fragment which contains a fully active catalytic site as judged by Ca^{2+}-ATPase activity but which exhibits very low actin-activated Mg^{2+}-ATPase activity. Comparing this fragment with fully active unphosphorylated myosin II, we found equivalent K_{ATPase} values (5 μM vs 4 μM) but a lower V_{max} (0.07 s^{-1} vs 1.9 s^{-1} per head). In the presence of ATP the head fragment exhibited a $K_{binding}$ of 5.6 μM which is higher than that of filamentous native myosin (0.3 μM) but might be equivalent to the binding of individual heads within the filament. After the head fragment was covalently crosslinked to actin in the absence of ATP, the actin-head complex hydrolyzed MgATP at a rate equivalent to V_{max} for the fully active unphosphorylated myosin II. We conclude that the actin-activated Mg^{2+}-ATPase activity of myosin II is regulated via a rate-limiting step in the catalytic cycle which depends on the conformation and/or orientation of the actin-associated myosin head. In intact myosin, the conformation and/or orientation of the heads may be determined by the conformation of the myosin filament as a whole which in turn is regulated by the state of phosphorylation of the individual myosin molecules.

T-AM-A11 MYOSIN-LINKED REGULATION AND SULFHYDRYL GROUPS. Margaret A. Titus & Andrew G. Szent-Györgyi. Department of Biology, Brandeis University, Waltham MA 02254.

The effect of sulfhydryl modification on the calcium sensitivity of scallop myosin was studied, using a variety of thiol-specific reagents. Scallop myosin was incubated overnight at 4 °C, at low ionic strength (40 mM NaCl, 5 mM Pi, 3 mM NaN_3, 1 mM $MgCl_2$, 0.1 mM EGTA, pH 7.0), with varying molar ratios of one of the following reagents: IAEDANS, NEM, iodoacetamide, mersalyl acid or PCMB. These reagents can be roughly divided into three groups on the basis of their effect on regulation. IAEDANS and NEM desensitized scallop myosin without the removal of regulatory light chains (R-LCs). Total loss of Ca^{2+}-sensitivity was achieved when 1 mole of IAEDANS was bound per head. The IAEDANS label was localized to the C-terminal 20K peptide of scallop myosin S-1. This demonstrates the involvement of an additional site on the heavy chain that is required for Ca^{2+} regulation, independent of R-LCs or the S-2 region. In addition, preliminary evidence suggests that rabbit myosin modified with IAEDANS, under identical conditions, is insensitive to regulation by troponin-tropomyosin. Iodoacetamide and PCMB activated the actomyosin ATPase while retaining sensitivity, whereas mersalyl acid neither desensitized nor activated the actomyosin ATPase. The high salt K·EDTA ATPase was specifically reduced by all of these reagents. Attempts to localize the reacted thiol groups are currently underway in order to define specific sites available for use in probe studies. Supported by NIH AM-15903 and MDA grants.

T-AM-A12 SEQUENCE ANALYSIS OF MOLLUSCAN MYOSIN LIGHT CHAINS. John H. Collins*, Winifred W. Barouch*, Ross Jakes§, John D. Leszyk*, Judith Spiegel#, Andrew G. Szent-Györgyi# and Janet L. Theibert*. *Dept. Biology, Clarkson Univ., Potsdam, NY 13676, §MRC Lab. Molec. Biol., Cambridge CB2 2QH (England), and #Dept. Biology, Brandeis University, Waltham, MA 02254.

We are analyzing the amino acid sequences of scallop essential light chain (SELC) and Mercenaria (clam) regulatory light chain (MRLC). Peptides derived from these proteins were separated by chromatography on Sephadex G-50 and by reverse-phase HPLC. Direct sequencing of the peptides was carried out with an automated, gas-phase protein sequencer. The sequence of SELC was determined by sequencing its five CNBr peptides. These were then aligned from studies on Met-containing tryptic and chymotryptic peptides. The sequence of MRLC is being determined from four peptides derived from cleavage at Arg with trypsin. We have sequenced the largest (58 residues) of these, and further studies are in progress. The single Cys of MRLC and the three Cys of SELC have all been placed. Potential Ca-binding sites have been identified. The results of these studies, in particular the locations of the Cys residues, will be used in our chemical cross-linking studies aimed at describing the behavior of these proteins in the myosin-linked Ca regulation of scallop muscle contraction. Supported by grants from the NIH (AM35120, AM15963), the NSF (DMB8510411) and the Muscular Dystrophy Association.

T-AM-B1 COMPARISON OF CA^{2+}-DEPENDENT SIGNALS OBTAINED WITH AEQUORIN, QUIN-2, FURA-2, AND CHLORTETRACYCLINE IN THE SAME SMOOTH MUSCLE CELLS. Tia T. DeFeo, James J. Ferguson and Kathleen G. Morgan. Harvard Medical School, Beth Israel Hospital, Boston, MA 02215.

The present study was initiated to investigate the possible use of multiple Ca indicators to give complementary information regarding Ca localization in different compartments of the same smooth muscle cells. Enzymatically isolated single cells from ferret portal vein (FPV) were loaded with the fluorescent dyes fura-2, quin-2 and chlortetracycline (CTC). FPV intact strips were loaded with aequorin. Quin and aequorin gave qualitatively the same cytoplasmic Ca signals when challenged with phenylephrine (PE) and potassium depolarization (K) although the initial spike of light caused by PE appeared blunted in the quin signals compared to the aequorin signal. When quin and aequorin signals (using equally effective concentrations of PE) were calibrated and plotted as the log $[Ca^{2+}]$ vs time, the traces appeared essentially identical. However, much higher concentrations of all agonists were necessary to produce contractions in quin loaded cells which were comparable to those in unloaded cells. CTC (which is thought to primarily reflect storage Ca) indicated a drop in Ca when challenged with caffeine, consistent with release of Ca from the stores. Fura signals were variable in the presence of caffeine but indicated a consistent rise in Ca during K. Aequorin signals consistently increased in a dose-related manner with increasing doses of caffeine. These results are consistent with the idea that aequorin and quin report cytoplasmic Ca^{2+}, CTC reports stored Ca and fura can report both. Support: NIH HL 31704 and an AHA Grant-In-Aid and Established Investigatorship.

T-AM-B2 INTRACELLULAR CA^{++} LEVELS IN PHORBOL ESTER-INDUCED CONTRACTION OF FERRET AORTA. Meei J. Jiang and Kathleen G. Morgan. Harvard Medical School, Beth Israel Hospital, Boston, MA 02215.

Previous studies on vascular smooth muscle in this laboratory have indicated that at steady-state there is a higher sensitivity of the contractile apparatus to $[Ca^{++}]_i$ in α-adrenergic receptor-mediated contractions than in K^+-induced contractions. In other cell types it has been suggested that phorbol esters activate protein kinase C at resting levels of intracellular Ca^{++}. Since phorbol esters have been shown to induce a tonic contraction in smooth muscle, we investigated the intracellular Ca^{++} levels in phorbol ester-induced contraction of ferret aortic smooth muscle. The bioluminescent protein aequorin, preloaded into aortic strips using a chemical loading procedure, was used as an intracellular Ca^{++} indicator. Intracellular calcium levels and isometric tension were measured simultaneously. The phorbol ester 12-deoxyphorbol 13-isobutyrate 20-acetate (DPBA, 0.5 μM) induced a slow contraction of 9.8 ± 1.6 mN force (n=6). An early small and transient increase in the aequorin signal, which appeared to be temporally dissociated from force development, was also observed. However, the force/Ca^{++} ratio at steady-state force was much higher than that of the K^+-induced contraction. Furthermore, 1 μM DPBA induced a contraction in Ca^{++} free - 2.5 mM EGTA Krebs buffer. The results of this study suggest that a phorbol ester sensitizes the contractile apparatus of vascular smooth muscle to Ca^{++} and that a significant amount of tension can be generated by the phorbol ester without influx of extracellular Ca^{++}. Whether the early Ca^{++} transient is correlated with the contraction induced by the phorbol ester is currently under investigation. Support: NIH HL 31704, AHA Grant-In-Aid, EI and AHA postdoctoral research fellowship.

T-AM-B3 DANTROLENE PREVENTS THE MALIGNANT HYPERTHERMIA SYNDROME IN SUSCEPTIBLE SWINES BY REDUCING THE MYOPLASMIC FREE $[Ca^{2+}]$. J.R. López, L. Alamo, D. Jones, P. Allen, L. Papp, J. Ryan and F. Sreter. Centro de Biofísica y Bioquímica, IVIC, Caracas, Venezuela. Dept. Anesth. Mass Gen. Hosp. Dept. Anesth. Brigham and Women's Hospital, Dept. of Muscle Res., Boston Biomedical Res. Int. Boston, MA 02114.

Malignant hyperthermia (MH) is a pharmacogenetic disorder of skeletal muscle triggered when susceptible patients or animals are exposed to volatile anesthetic agents and/or depolarizing muscle relaxants. We have used Ca^{2+} selective microelectrode (López *et al.*, Biophys. J. 43:1, 1983) to measure *in vivo* the intracellular free Ca^{2+} concentration in skeletal muscle of MH susceptible swines before and after Dantrolene (D) administration. We have investigated the effectiveness of (D) in preventing clinical MH and the relationship between the resting $[Ca^{2+}]_i$ and the probability to induce the MH syndrome. The swine were anesthetized and the $[Ca^{2+}]_i$ was measured as described previously (López *et al.*, Biophys. J. 47:313a, 1985). The resting intracellular free $[Ca^{2+}]$ was 0.38 ± 0.2 μM (M ± SEM), which agrees with our previous measurements in susceptible swine (López *et al* Muscle and Nerve in press).

The administration of 0.5, 1, 2, 2.5 and 3 mg/Kg (D) reduced the $[Ca^{2+}]_i$ to 0.30, 0.21, 0.08, 0.11, and 0.09 μM respectively. The 0.5 mg/Kg dose of (D) failed to prevent the MH syndrome after exposure to halothane (2% for 30 minutes) and succinylcholine (2 mg/Kg IV). The 1 mg/Kg dose was sufficient to prevent the clinical syndrome in 2 out of 3 animals, and the 2.5 mg/Kg dose was uniformly protective in 4 animals. These results suggest that the mechanism by which (D) protects susceptible animals exposed to triggering agents is by reducing the intracellular free $[Ca^{2+}]$. (Supported by CONICIT S1-1277, M.D.A., NIH GM 15904).

T-AM-B4 SKELETAL MUSCLE FIBRES FROM FAST-TWITCH MUSCLES IN THE RAT ARE MORE SUSCEPTIBLE TO MECHANICAL INACTIVATION THAN FIBRES FROM SLOW TWITCH MUSCLES. Angela F. Dulhunty and Michael Chua (Intr. by Ian Neering). Department of Physiology, John Curtin School of Medical Research, Australian National University, P.O. Box 334 Canberra, A.C.T. 2601, Australia.

Depolarization of skeletal muscle leads to mechanical activation followed by inactivation. The voltage dependence of activation differs in mammalian fast- and slow-twitch fibres, being shifted to more negative potentials in slower fibres (Dulhunty & Gage, J. Physiol. 341, 213-231, 1983). In this study we explored the possibility that the voltage dependence of inactivation is correlated with the isometric contraction time of fibres from rat fast-twitch (extensor digitorum longus, e.d.l.) and slow-twitch (soleus) muscles. A two microelectrode voltage clamp technique was used to examine the effect of membrane potential on contraction threshold for a 15msec test pulse. There was an increase in contraction threshold as a result of inactivation when the holding potential was depolarized from -80mV. Potassium (K-) contractures were used to examine steady-state inactivation which was seen as a reduction in the tension produced by a sudden test exposure to 200mM potassium following depolarization by conditioning exposures to potassium concentrations that were higher than normal (3.5mM) but less than 200mM. The two techniques yielded similar results. E.d.l. fibres, in contrast to soleus, showed more inactivation with less depolarization. On average, e.d.l. fibres were fully inactivated at -30mV and partial inactivation was apparent at -69mV. On the other hand, soleus fibres were not fully inactivated until the holding potential was reduced to -20mV and no inactivation was seen until the fibres were depolarized to -40mV.

T-AM-B5 **DOES THE ACCUMULATION OF H^+ OR INORGANIC PHOSPHATE EXPLAIN EARLY CONTRACTILE FAILURE DURING HYPOXIA?**

H. Kusuoka, W. Jacobus, M.L. Weisfeldt, and E. Marban, Department of Medicine, The Johns Hopkins Medical Institutions, Baltimore, MD 21205

The depression of contractility which develops rapidly during hypoxia is not associated with a decrease in activator Ca^{2+} (Allen & Orchard, J. Physiol., 1983) although H^+ and/or inorganic phosphate (Pi) accumulation may play a role by depressing maximal Ca-dependent force. We tested this hypothesis by measuring pressure and ^{31}P NMR spectra in Langendorff-perfused ferret hearts at 30°C. Tetanus, a plateau of developed pressure, was elicited by right ventricular pacing at 10 Hz after exposure to ryanodine (1-5 uM). Maximal Ca-dependent pressure (MCP) was identified by the saturation of pressure with respect to $[Ca]_o$ observed during tetani as $[Ca]_o$ was increased to 10-15 mM in HEPES-buffered, 100% O_2-bubbled perfusate and during hypoxia induced by bubbling with N_2. Two tetani were elicited during acquisition of each spectrum as an indication of MCP. An inverse linear correlation was observed between [Pi] and MCP ($r=-0.89$, $n=12$), with a 13.7% decline in pressure per 1 umole/g wet wt increase in [Pi]. pH_i did not show a significant correlation with MCP ($r=0.41$). As another means of relating [Pi] and MCP, we investigated the 24.9% decline of pressure ($n=8$) observed during tetani maintained for 6 sec. NMR pulses were applied at peak pressure (1 sec) and 4.7 sec afterwards to yield spectra early and late during tetani. The relationship between [Pi] and MCP obtained in this manner was identical to that during hypoxia, and the lack of correlation with pH_i was confirmed. The data are consistent with a modulation of maximal Ca-dependent pressure by [Pi] but not pH_i.

T-AM-B6 IS Ca/H EXCHANGE INVOLVED IN t-SR COUPLING? Brian A. Curtis
Univ of Illinois College of Medicine at Peoria, Peoria, IL 61656

The recovery reaction following a K contracture is thought to reset the t-SR coupling step. This rate can be assessed by the ratio of areas under the time-tension curves of two contractures separated by 10-75 sec in normal Ringer. Bundles of 1-7 fast fibers from frog semi-tendinosis or tibialis muscles were rapidly flushed with 190 mM potassium methanesulfonate. The data, Log (100-%recovery) plotted as a function of time, can be fitted by a straight line; suggesting first order kinetics. The average time constant was 34+-3 sec (11) at 15 C and had a Q 10 of 2.06. 10 min at pH 6.3 prior to the contractures slowed ($p<.01$) the recovery reaction to a time constant of 48 +- 3 sec (6) at 15 C. At low pH the final rate constant of decay of contracture tension was unchanged; the rate of Ca sequestration by the SR was not altered by transient low pH. The rate of rise of tension was, however, slowed and the duration of the tension plateau was reduced. Both of these relate to the coupling between membrane depolarization and Ca release by the SR, as does the rate of recovery of the ability to do the succeeding contracture. These results suggest that t-SR coupling may involve one "external" Ca and 3 "internal" H changing their orientation within the t membrane upon depolarization. These ions moving off their binding sites would be recorded as charge movement and the "internal" Ca could trigger Ca induced Ca release from the SR.

T-AM-B7 REVERSAL OF ELECTRICALLY-GUIDED EPIDERMAL CELL MOVEMENT WITH CALCIUM CHANNEL ANTAGONISTS PLUS IONOPHORE A23187. Mark S. Cooper and Manfred Schliwa, Department of Zoology, University of California, Berkeley CA 94720 (Intro. by H. J. Bremermann).

Fish epidermal cells migrate at rates of 20 – 60 μm/min toward the cathode in DC electric field of 0.5 – 15 V/cm. The cells (typically 20x40 μm), which migrate perpendicular to their long axis, extend broad lamellipodia in their direction of movement. Previously, we have found that both spontaneous and electrically-guided epidermal cell movement are reversibly blocked by a variety of Ca^{2+} channel antagonists such as 1 mM La^{3+}, 10 mM Co^{2+}, 50 μM verapamil, or 50 μM nitrendipine (Cooper and Schliwa, J. Neurosci. Res 13 (1985) 223). Recently, we have discovered that cells paralyzed by Co^{2+} or verapamil can be reactivated by 5 – 20 μM calcium ionophore A23187. These reactivated cells, however, show a distinct reversal of electrically-guided movement, migrating toward the anode instead of the cathode. A23187 alone at 5 – 20 μM does not produce this reversal of polarity. These results strongly suggest that an asymmetry of Ca^{2+} influx through the cell's endogenous Ca-channels is the factor which determines cell polarity during cathode-directed galvanotaxis. This asymmetry is the only factor which should be removed when the cells are paralyzed by Co^{2+} or verapamil and subsequently reactivated with A23187. We propose that the asymmetry of Ca^{2+} influx which appears to control cathode-directed epidermal cell migration arises from an increased Ca-conductance of the cathode-facing (depolarized) cell membrane. A23187 within the cell membrane may accumulate on the anode-facing side of the cell by electrophoresis since the ionophore is negatively charged when deprotonated. Such an asymmetry of ionophore may be the guiding cue for anode-directed migration once Ca^{2+} influx through the cell's intrinsic Ca-channels is blocked.

T-AM-B8 LEVELS OF INOSITOL PHOSPHATES IN STIMULATED AND RELAXED MUSCLES. K. Asotra* and J. Vergara, Dept. of Physiology, UCLA School of Medicine.

It has been previously reported that soluble extracts from electrically stimulated muscles incubated with [^{3}H] myo-inositol contain greater amounts of [^{3}H] labelled inositol phosphates as compared to unstimulated controls (PNAS 82:6352-6356,1985). We have extended these studies using high performance liquid chromatography (HPLC) instead of the conventional Dowex columns. Aqueous extracts of fast frozen stimulated and control sartorii and semtendinosii muscles of Rana catesbeiana were injected into a uBondapak-NH_2 column equilibrated with 60 mM Acetic Acid/Ammonium Acetate, pH 4, and eluted isocratically for 20 min followed by a linear gradient up to 2M Acetic Acid/Ammonium Acetate at a flow rate of 1 ml/min. The elution fractions were counted for [^{3}H] label and analysed for organic phosphorus content (after removal of endogenous nucleotides by enzymatic hydrolysis or adsorption on activated charcoal) to identify and quantitate mainly $InsP_2$ and $InsP_3$. Our results indicate that control muscles contain less than the detection limit of 0.3 nmoles of $InsP_3$/g fresh muscle weight. This concentration increases to at least 8 nmoles/g when frozen after 20 sec of tetanic stimulation (50 Hz). $InsP_2$ is present at about 20 nmoles/g in resting muscles and increases to about 80 nmoles/g at the end of 20 sec tetanii. A relaxation period of 2 sec after a tetanus resulted in total disappearance of $InsP_3$ and a reduction of $InsP_2$ to one-half maximal. Supported by grants from USPHS (AM 25201) and MDA.

T-AM-B9 INOSITOL (1,4,5) - TRISPHOSPHATE-INDUCED RELEASE OF Ca^{2+} FROM THE SARCOPLASMIC RETICULUM OF SKINNED CARDIAC CELLS. A. Fabiato, Medical College of Virginia, Richmond, VA 23298

Inositol (1,4,5)-trisphosphate ($Ins(1,4,5)P_3$) induced a release of Ca^{2+} from the sarcoplasmic reticulum (SR) of skinned cardiac cells from the adult rat ventricle (5-6 μm thick, 7-8 μm wide, and 35-45 μm long). The solutions were changed within 1 ms, and were at pMg 2.50, pMgATP 2.50, pH 7.10, and 22°C. The Ca^{2+} release was detected either in the presence of a low Ca^{2+} buffering (0.10 mM total EGTA or 0.05 to 0.20 mM Br_2BAPTA) with recording of tension and aequorin light transients, or in the presence of a high Ca^{2+} buffering (10 mM total EGTA) with a subsequent application of caffeine in the presence of 0.2 mM total EGTA to measure the Ca^{2+} content of the SR. The amplitude of the Ca^{2+} release increased from 3 to 10-15% of maximum tension when [$Ins(1,4,5)P_3$] was increased from 2 to 30 μM. The rate of total calcium release induced by 30 μM $Ins(1,4,5)P_3$ was 0.12 mmol $.s^{-1}$ per liter of cell water accessible to aequorin and Ca^{2+}, which was 13 times less than the rate of total calcium release elicited by an optimum Ca^{2+}-induced Ca^{2+} release (CICR). Simultaneous stimulation by CICR (increase of [free Ca^{2+}] from pCa 7.75 to pCa 6.25 in 1 ms) and 30 μM $Ins(1,4,5)P_3$ resulted in two distinct transients of aequorin light and tension: the $Ins(1,4,5)P_3$-induced Ca^{2+} release occurred much after the CICR. This suggests that $Ins(1,4,5)P_3$-induced release of Ca^{2+} from the SR is less likely than CICR to be the physiological mechanism of cardiac excitation-contraction coupling. $Ins(1,4,5)P_3$-induced release of Ca^{2+} strongly potentiated the spontaneous cyclic release of Ca^{2+}, which occurs when the SR is overloaded with Ca^{2+}, and was strongly potentiated by caffeine, but was not affected by decreasing the [free Mg^{2+}]. $Ins(1,4,5)P_3$ (up to 200 μM) had no effect on the myofilaments or the mitochondria. (I thank J. W. Putney for advice and gift of $Ins(1,4,5)P_3$.)

T-AM-B10 INOSITOL 1,4,5-TRISPHOSPHATE INDUCES FORCE GENERATION OF PEELED SKELETAL MUSCLE FIBERS AT 10^{-3}M FREE MG^{2+}. Sue K. Donaldson, Nelson D. Goldberg, Timothy F. Walseth, and Daniel A. Huetteman. University of Minnesota, Minneapolis, MN 55455.

Inositol 1,4,5-trisphosphate (IP_3) elicits isometric force generation and net ^{45}Ca efflux from nonmitochondrial internal stores of mechanically peeled (sarcolemma removed) rabbit adductor magnus muscle fibers (manuscript submitted). At 1mM free Mg^{2+}, 1μM IP_3 had a maximum effect if it was microinjected into the myofibrillar space of the peeled fiber immersed in silicone oil. In contrast to the effectiveness of IP_3, IP_2 (1mM) yielded little or no response and 1μM IP_1 had no effect. These experiments were conducted under conditions of high [Cl^-] (66mM) to assure that any sealed transverse tubules (TTs) were depolarized. Here we report that 1nl 1μM IP_3 injected into the myofibrillar space of peeled rabbit soleus fibers (in the presence of oligomycin to block mitochondrial Ca^{2+} transport) is effective in eliciting isometric force generation at 1mM free Mg^{2+}. The normalized peak magnitude of the IP_3-induced force generation, evidenced as end-to-end tension in fibers 2-3mm long, was the same when stimulated by 1μM microinjected IP_3 in presence or absence of a 20mM procaine block of the caffeine (10mM) contracture in the same soleus fiber; this suggests that the Ca^{2+} release response is not propagated via Ca^{2+}-induced SR Ca^{2+} release. It was also possible to elicit IP_3-induced force generation immediately prior to and following Cl^--induced isometric force transients, suggesting that exogenous IP_3 acts at a step beyond TT depolarization. This study was supported by USPHS, NIH grants AM 35132 and GM 28818.

T-AM-B11 INOSITOL TRISPHOSPHATE ENHANCES Ca^{2+} RELEASE FROM THE SARCOPLASMIC RETICULUM OF SKINNED CARDIAC AND SKELETAL MUSCLE. T.M. Nosek, W.F. Williams, S.T. Zeigler, and R.E. Godt (Intr. by K. Green). Dept. of Physiology, Medical College of Georgia, Augusta, GA. 30912-3376

The level of intracellular Ca^{2+} is important in regulating a variety of cellular functions. Many receptor agonists that increase intracellular Ca^{2+} are believed to do so by stimulating D-myo-inositol 1,4,5-trisphosphate (IP3) production from plasmalemmal phosphatidylinositol-4,5-bisphosphate inasmuch as intracellular IP3 levels are increased by these agonists and IP3 in physiological concentrations can release Ca^{2+} stored in the endoplasmic reticulum. Recent experiments from other laboratories suggest that IP3 may also be involved in the excitation-contraction coupling process of cardiac and skeletal muscle cells. Our results support this hypothesis. We used small fiber bundles (100-200 μM diameter) from guinea pig papillary muscles skinned with saponin (50 ug/ml). We find that Ca^{2+}-induced force oscillations, observed in solutions with pCa 7.0 and containing low EGTA (0.05 mM), are enhanced in magnitude and frequency by IP3 at concentrations as low as 1 uM. Similarly, IP3 at 10 uM can induce such oscillations in mechanically skinned frog skeletal muscle. Moreover, in skinned cardiac fibers IP3 increases the magnitude of caffeine contractures at submaximal caffeine concentrations to a greater extent than at near maximal caffeine concentrations. IP3 (30 uM) does not affect the Ca^{2+} sensitivity or maximum force generated by skinned cardiac muscle. We conclude that IP3 enhances the Ca^{2+}-induced release of Ca^{2+} from the sarcoplasmic reticulum, possibly from the same pool and through the same mechanism as caffeine.

T-AM-B12 PERCHLORATE POTENTIATES THE STIMULATION OF SKINNED MUSCLE FIBERS BY ION GRADIENTS. Elizabeth W. Stephenson, Dept. of Physiology, UMDNJ-NJ Medical School, Newark, NJ 07103

Recent work suggests that mechanically skinned fibers can be activated by T-tubule depolarization and this is the primary effect of depolarizing ion gradients at constant [K] [Cl]. The present studies examined potentiation of this stimulus by perchlorate (ClO_4^-), which shifts the voltage dependence of intramembrane charge movements associated with contractile activation (Luttgau et al, Biophys. J. 43:247, 1983). ^{45}Ca efflux and isometric force were measured in mechanically skinned segments of frog semitendinosus fibers at 19°C. All solutions contained 120 mM major salt, 5 mM Na_2ATP, 5 mM $MgSO_4$, 10 mM imidazole, pH 7.0. Segments loaded with ^{45}Ca and rinsed in dilute EGTA solutions were stimulated by choline (ch) Cl replacement of K methanesulfonate (Mes) at constant [K][Cl]. In interrupted responses (5 mM EGTA added in <2 s to minimize reaccumulation), 120 mM chCl caused rapid contraction and release of ∿30% fiber ^{45}Ca in ∿1 min. Control loss in KMes, 5 mM EGTA was 5%. Release in 60 mM chCl was only 6% and ClO_4 effects were erratic. Release in 70 mM chCl increased significantly to 9% ^{45}Ca; 8 mM tris ClO_4 increased this release to 14%, potentiating stimulation (above control loss) more than 2-fold. Preliminary results suggest that ClO_4 potentiated the small Ca^{2+}-insensitive component of ionic stimulation in EGTA (Biophys. J. 41:231a, 1983), which was minimal under present conditions. ClO_4 alone was ineffective. These results show that submaximal ^{45}Ca release from skinned fibers stimulated by ionic depolarization is potentiated by an agent thought to act on T-SR coupling, and suggest that coupling can be studied in this preparation. Supported by NIH Grant AM 30420.

T-AM-C1 PSEUDOMONAS EXOTOXIN A: MEMBRANE BINDING, INSERTION AND TRAVERSAL. Zohreh Farahbakhsh, Rae Lynn Baldwin and Bernadine J. Wisnieski. Dept. of Microbiology and the Molecular Biology Institute, University of California, Los Angeles, CA 90024.

Recently we described the effects of low pH and cleavage on Pseudomonas toxin (PTx) binding, insertion, and pore formation [Infect. Immun. 50, in press]. Now, with vesicle targets, we have established that PTx binding increases with increasing ionic strength and temperature, reaches a maximum within 10 min, and is optimal with negatively charged vesicles. When toxin insertion was assayed by photolabeling with the intramembranous probe 12-(4-azido-2-nitrophenoxy)stearoyl-1-^{14}C-glucosamine and the data reduced to labeling efficiencies per μg of bound toxin, we found that while the amount of PTx bound to vesicles increased with increasing temperature, the proportion that was photolabeled decreased. This suggested that PTx traverses the membrane faster at higher temperatures and hence less is accessible to the probe when the samples are irradiated. Such an explanation seems reasonable because the time course of photolabeling revealed a steady decrease after 10 min while the amount of vesicle-bound PTx showed only a slight decline. Toxin-membrane traversal was demonstrated by incubating PTx with trypsin-loaded vesicles, dropping the pH to 4, irradiating, and raising the pH back to 8 (where toxin binding is negligible). Three major fragments were observed. Since all bore photolabel, it appears that PTx traverses the membrane as a unit structure. We propose that the PTx entry process involves an acid-induced change in conformation that favors membrane binding and insertion, and that the traversal kinetics are governed by the physical properties of the bilayer. Supported by USPHS GM22240 and the UCLA Academic Senate.

T-AM-C2 OPTICAL STUDIES OF THE INTERACTION OF BEE VENOM MELITTIN WITH PHOSPHOLIPIDS. Thomas D. Bradrick, Jean-Louis Dasseux, Mohamed A. Abdalla, and Solon Georghiou, Biophysics and Chemical Physics Lab., Dept. of Physics, University of Tennessee, Knoxville, TN 37996-1200.

We have studied the interaction of melittin with DMPC unilamellar and multilamellar vesicles at a protein-to-lipid molar ratio of 1/60 with steady-state and nanosecond fluorometry using pyrene and DPH as fluorescent probes as well as with laser Raman spectroscopy. We used melittin highly purified by HPLC to avoid any effects from any residual phospholipase A_2 activity. The protein is found to induce an increase in the intermolecular order of the acyl chains of unilamellar vesicles below, at, and above T_t and to decrease strongly the diffusion rate, D_w, only below T_t. On the other hand, for multilamellar vesicles, the protein induces a decrease in the order only in the vicinity of T_t but it does not affect D_w appreciably. These effects are consistent with the observed changes in the degree of enhancement of the 0-0 vibronic transition of pyrene. Moreover, the protein broadens the thermal transition profile of multilamellar vesicles but sharpens dramatically that of unilamellar vesicles. The latter effect is interpreted as arising from a large change in the supramolecular lipid state which we also observed by DSC and analytical ultracentrifugation. For the tetrameric form of melittin, which prevails at the high melittin concentration necessitated by Raman spectroscopy, we find that the protein: (i) decreases the intramolecular order of the chains below T_t and increases it above T_t (based on measurements in the C-C region); and (ii) induces similar effects in the temperature profile in the C-H region which reflects both intra- and intermolecular interactions.

T-AM-C3 THE EFFECT OF GRAMICIDIN A' ON PHOSPHOLIPID BILAYERS. B.A. Cornell, CSIRO, PO Box 52, North Ryde, NSW, 2113, Australia.

The purpose of this communication is to examine the controversial claim that high concentrations of gramicidin A' cause disorder within the L_α phase of phosphatidylcholine-water dispersions. Solid-state nuclear magnetic resonance, (NMR), density gradient and X-ray diffraction techniques are used to confirm the existence of such an effect and a model is proposed which identifies the mechanisms of the interaction of the gramicidin A' with phospholipid membranes. According to this model, the addition of gramicidin A' influences the motion of the surrounding lipids via two independent mechanisms. The first is an increase in the phospholipid headgroup spacing due to the intercalation of the polypeptide into the hydrocarbon region of the bilayer. The relatively small polar region of gramacidin A' occupies less volume per unit area of the membrane than does the phospholipid. The reduced density of packing in the polar region causes a decrease in order of the phosphate group and is balanced by an increase in the density of packing of the hydrocarbon moiety. This increase in packing density produces an increase in the order detected by carbon-13 NMR of the carbonyl groups and by deuterium NMR of the hydrocarbon chains. The second effect which dominates at higher concentrations of gramicidin A' causes a reduction in order at all levels of the bilayer and arises due to a drop in surface tension when lipid is substantially bounded by gramicidin A'. The model accounts for the currently available NMR, X-ray diffraction and surface, monolayer studies. The model also accounts for the ability of gramicidin A' to trigger a transition of the lipid from the lamellar to hexagonal II phase and for the concentration dependence of this transition on the length of the lipid chain.

T-AM-C4 **COMPARISON OF GRAMICIDIN A/LIPID DISPERSIONS AND CO-CRYSTALS BY RAMAN SCATTERING.** Kurt W. Short, Richard Myers, Stephen P. A. Fodor and A. Keith Dunker, Biochemistry/Biophysics Program and Dept. of Chemistry, Washington State Univ., Pullman, WA 99164-4660 and B. A. Wallace, Dept. of Biochemistry and Molecular Biophysics, Columbia Univ., 630 West 168th Street, New York, NY 10032.

Laser Raman spectra are presented for gramicidin A crystals, gramicidin A/DMPC dispersions and gramicidin A/DMPC co-crystals. The relative intensities of the choline (716 cm^{-1}) and tryptophan (756 cm^{-1}) Raman peaks indicate that the co-crystals contain two lipids for each gramicidin A molecule. This result is confirmed by chemical assays on washed crystals.

Below the lipid phase transition temperature and at high lipid:protein ratios (e.g., 25:1), the lipid is ordered in the dispersions but becomes increasingly disordered as the lipid:protein ratio is lowered. In contrast to this trend, and despite the low (2:1) lipid:protein mole ratio, the co-crystals have highly ordered lipids that possibly contain no gauche bonds at all.

The amide I peak position near 1670 cm^{-1} is found to be independent of the lipid:protein ratio, indicating β-structured protein at all ratios. However, the amide I is found to broaden significantly at low lipid:protein ratios and to broaden still further in the co-crystals, suggesting that protein-protein interactions induce band-broadening distortions of the local hydrogen bonding structure.

T-AM-C5 BINDING OF HEMAGGLUTININ TO SUPPORTED PHOSPHOLIPID BILAYERS

E. E. Uzgiris, General Electric Research and Development Center, Schenectady, N.Y. 12301

Bromaline released influenza hemagglutinin undergoes a conformation change at $pH_1$5.0 that exposes a hydrophobic domain which at higher pH is sequestered in the interior space of the molecule[1]. I find that under certain conditions, this low pH form of hemagglutinin can bind to supported phospholipid bilayers composed, either, of phosphatidylcholine or phosphatidylethanolamine or GM_1 gangliosides. This binding is receptor free and requires the maintenance of pH5 during the incubation procedure. It is likely that the binding occurs through the insertion of the hydrophobic domain into the bilayer. Other proteins, e.g. goat antibodies, human IgG, do not bind to the bilayers at all for identical conditions. The bound hemagglutinin does not form ordered 2-D crystals in the experiments reported but does form dense close packed structures as seen in the electron micrographs of the specimens. Optical diffraction of the micrographs gives a diffuse ring corresponding to a distance of about 120 Å between nearest neighbor stain exclusion peaks. This high density binding is not observed at 23°C, is partial at about 28°C, and is complete at 37°C, for a phosphatidylcholine bilayer and 150mM NaCl. Increased ionic strength promotes the observed binding while decreasing the ionic strength retards it. Furthermore, the low pH form of hemagglutinin is unable to bind if the pH is brought back up to pH7. Prospects for inducing ordering in the hemagglutinin monolayers will be discussed.

I thank Don Wiley and John Skehel for providing the hemagglutinin samples.

[1] J.J. Skehel et. al. Proc. Natl. Acad. Sci USA 79 968 (1982)

T-AM-C6 INTERACTION OF PHOSPHOLIPASE A_2 WITH NOVEL SHORT-CHAIN LECITHIN/LONG-CHAIN PHOSPHOLIPID VESICLES. N. Elise Gabriel, Nike V. Agman, and Mary F. Roberts, Department of Chemistry, M.I.T., Cambridge, MA 02139

The interfacial activation of phospholipase-A_2 (PLA_2) has been examined using short-chain lecithin micelles and stable unilamellar vesicles (SLUVs) formed spontaneously upon mixing small amounts of short-chain lecithin and long-chain phospholipid. Extensive characterization of SLUVs using NMR spectroscopy and negative stain EM reveals that this method of vesicle preparation can produce bilayer vesicles spanning 100-1000 Å depending on the identity of the lipids and the ratio of the two components. Relatively small unilamellar vesicles are produced from the combination of short-chain lecithin and long-chain phospholipid in its gel state, while large vesicles are produced when the long-chain phospholipid is liquid crystalline. The activity of cobra venom PLA_2 towards SLUVs has been examined as a function of long-chain phospholipid and temperature. The short-chain component is the preferred substrate in these vesicles and is hydrolyzed at a rate ∿ 10 times that of the long-chain component. The specific activity of PLA_2 towards diheptanoyl-PC micelles does not vary dramatically with temperature over the range 15-45°C. When incorporated in vesicles with dipalmitoyl-PC (DPPC) the hydrolysis of diheptanoyl-PC shows a pronounced temperature dependence: below the T_m of DPPC the specific activity of PLA_2 is constant; as the temperature approaches the T_m, the activity increases dramatically; above T_m activity decreases. A correlation of kinetic rates with vesicle sizes shows that PLA_2 prefers the diheptanoyl-PC substrates in small rather than large vesicles. These results imply that the length of the fatty acid in the long-chain component and vesicle curvature are critical in understanding the interfacial behavior of PLA_2.

T-AM-C7 FLUORESCENCE OF CYTOCHROME b_5 IN VESICLES WITH AN ASYMMETRIC DISTRIBUTION OF BROMINATED PHOSPHATIDYLCHOLINE. Peter W. Holloway, James Everett, Adam Zlotnick, and Joan Tennyson. Dept. of Biochemistry, Univ. of Virginia Sch. Med. Charlottesville, VA 22908

The fluorescence of cytochrome b_5, which emanates from the tryptophan in the hydrophobic membrane-binding domain, is quenched when the protein binds to small unilamellar vesicles made from 1-palmitoyl-2-(6,7-dibromostearoyl)phosphatidylcholine (6,7 BRPC). By use of phosphatidylcholine-specific exchange protein, vesicles were made which contained the 6,7 BRPC in either the outer or inner monolayer of the vesicle. The asymmetric vesicles were isolated by sucrose density gradient centrifugation, in which they banded at a sucrose density consistent with their expected, and confirmed, composition. The vesicles were shown to have the expected asymmetric distribution of 6,7 BRPC by monitoring the fluorescence of an externally added amphipathic carbazole compound. In other experiments is was shown that this carbazole compound, when uniformly incorporated into vesicles by co-sonication, would only exchange to other vesicles in proportion to the amount in the outer monolayer of the original donor vesicle and could not flip-flop. When cytochrome b_5 was added to the vesicles which had an asymmetric lipid composition, the tryptophan fluorescence was maximally quenched when the vesicles had a high concentration of 6,7 BRPC in the outer monolayer and was minimally quenched when the vesicles had a high concentration of 6,7 BRPC in the inner monolayer. These data, together with previous studies, suggest that the tryptophan which is quenched by the 6,7 BRPC is located 0.7 nm below the outer surface of the phosphatidylcholine vesicle. Supported by GM 23858.

T-AM-C8 PROTON-NMR STUDIES AT 500 MHZ OF THE INTERACTION OF D-β-HYDROXYBUTYRATE DEHYDROGENASE (BDH) WITH PHOSPHOLIPID (PL) VESICLES CONTAINING PHOSPHATIDYLCHOLINE (PC). Alan Deese[+], J. Oliver McIntyre*, Edward Dratz[+], Perry Churchill* and Sidney Fleischer*, [+]Chemistry Dept. Univ. Calif. Santa Cruz, Santa Cruz, CA 95064, and Dept. of Molecular Biology, Vanderbilt University, Nashville, TN 37235.

BDH is a lipid-requiring enzyme that specifically requires PC for enzymic activity. When BDH is added to PL vesicles (ternary mixture of PC:N,N-dimethyl-phosphatidylethanolamine:phosphatidylpropan-1,3-diol; 1:4:1 molar ratio) at a ratio of one BDH monomer per 4-6 PC, the outside choline N-methyl resonance is broadened, whereas the inner PC resonance remains essentially unaffected. The interaction appears to be selective for PC. These observations are interpreted as showing that BDH is an amphipathic molecule which inserts unidirectionally into the outer monolayer and does not gain access to the PC headgroups at the inner surface. BDH interacts strongly with the choline N-methyl region and inhibits the motion of this segment of the PC headgroup, reflecting the polar phospholipid specificity of the enzyme. By contrast, BDH does not perturb the hydrophobic proton resonances of the PL (vinyl, -(methylene)$_n$, terminal methyl) indicating that the primary interaction is at the polar region of PC.

When the ratio of PC to BDH is increased, we find that one BDH tetramer perturbs many PC molecules (in excess of 100). This means that BDH forms complexes with PC which dissociate repeatedly within the time-frame of NMR sensitivity ($\sim 10^5$/sec). The NMR studies were carried out at a concentration of PC in the vesicle which gives optimal activation. When the mole fraction of PC is decreased while maintaining the same total PL content, BDH function is proportionately reduced. The active BDH-PC complex is considered to be in a dynamic equilibrium, so that the amount of active enzyme is dependent on both the "on rate" and "off rate" of PC association. These studies suggest that at limiting PC concentration in the vesicle, the formation of the BDH complex with PC, which is bimolecular, becomes collision limited. (Supported in part by grants from NIH: AM 14632, EY00175).

T-AM-C9 LIPID-PROTEIN INTERACTIONS IN CYTOCHROME c OXIDASE. A COMPARISON OF COVALENTLY ATTACHED PHOSPHOLIPID PHOTO-SPIN LABEL WITH LABEL FREE TO DIFFUSE IN THE BILAYER O.H. Griffith, D. A. McMillen, J.F.W. Keana, P.C. Jost, J.J. Volwerk, and R.J. Mrsny, Institute of Molecular Biology and Department of Chemistry, University of Oregon, Eugene, OR 97403.

The aim of this study was to clarify the possible origins of the motion-restricted ESR spectral component observed in membranes. For this purpose, a phospholipid photo-spin label was synthesized, characterized, and used to study lipid-protein interactions in beef heart cytochrome c oxidase. The probe was designed with a nitroaryl azide incorporated in the phospholipid head group, and a spin label on the sn-2 side chain, and was radiolabeled. Upon photolysis, the photo-spin label reacted with the protein in high yields (50% attached). ESR spectra of the attached labels at 25 °C indicated a constant fraction of motion-restricted lipid chains, independent of the lipid to protein ratio. In contrast, a spin-labeled phosphatidylcholine and the pre-photolyzed photo-spin label, both free to diffuse in the bilayer, exhibited behaviour in agreement with the multiple equilibria binding model. These results, as well as data obtained with membranes frozen at -196 °C, show how several situations that lead to a motion-restricted ESR line shape can be distinguished. This study provides additional evidence that the fraction of lipids normally in contact with protein, and not aggregation artifacts, accounts for the observed motion-restricted component of ESR spectra of reconstituted cytochrome c oxidase in phospholipid bilayers. In a separate approach, the multiple equilibrium binding treatment developed previously has been extended to membrane proteins solubilized in detergents, resulting in a better understanding of the thermodynamics, of lipid-protein interactions. Supported by NIH Grants GM 25698 and 34916.

T-AM-C10 ^{31}P NMR STUDIES OF LIPID-PROTEIN INTERACTIONS IN ROD OUTER SEGMENT AND SARCOPLASMIC RETICULUM MEMBRANES. Jeffrey F. Ellena, Robert D. Pates, and Michael F. Brown. Department of Chemistry and Biophysics Program, University of Virginia, Charlottesville, VA 22901.

We have continued our ^{31}P NMR studies of ROS and SR membranes (1) and still find no evidence for observable or unobservable broad spectral components due to protein-induced lipid immobilization. Two further series of experiments have been performed. First we have selectively saturated spectral regions lying just outside the typical liquid crystalline bilayer (L_α phase) spectra of the ROS and SR membranes using the DANTE pulse sequence. No loss of intensity attributable to exchange between the bilayer (L_α phase) component and a putative broad component due to protein-induced lipid immobilization was observed. This disagrees with results obtained by Selinsky and Yeagle (2) for SR membranes. Second, we have obtained spectra of ROS and SR membranes using a solid-state NMR spectrometer capable of recording rigid limit (i.e. very broad) ^{31}P NMR spectra with minimal distortion. Broad spectral components similar to those observed by Yeagle and collaborators (3,4) were not seen, in agreement with several other studies (1,5). The nature and extent of the influences of rhodopsin and the Ca^{2+} ATPase on lipids in the ROS and SR membranes will be discussed. (1) R.D. Pates et al., Biophys. J. 47, 492a (1985). (2) B.S. Selinsky and P.L. Yeagle, BBA 813, 33 (1985). (3) B.S. Selinsky and P.L. Yeagle, Biochemistry 23, 2281 (1984). (4) A.D. Albert and P.L. Yeagle, PNAS 80, 7188 (1983). (5) I.C.P. Smith and I.H. Ekiel, in ^{31}P NMR-Principles and Applications, p 447 (1984). Work supported by NIH Grant EY03754, postdoctoral fellowships from the NIH (J.F.E.) and American Heart Association Virginia Affiliate (R.D.P.), and by an RCDA from the NIH (M.F.B.). M.F.B. is an Alfred P. Sloan Research Fellow.

T-AM-C11 CONFORMATIONS OF SIGNAL SEQUENCES IN LIPID MONOLAYERS FROM ATR FT-IR AND CD SPECTROSCOPIES. R.A. Dluhy[1], D.G. Cornell[2], M.S. Briggs[3], and L.M. Gierasch[3]. [1]Batelle Laboratories, Columbus, Ohio 43210; [2]Eastern Regional Research Center, USDA, Philadelphia, Pennsylvania 19118; [3]Department of Chemistry, University of Delaware, Newark, Delaware 19716.

Signal sequences are N-terminal extensions present on proteins destined to be secreted from cells. Required for export, their roles in protein translocation are poorly understood. Since interactions of signal sequences with phospholipids are likely in vivo, we have investigated the affinity of signal peptides for phospholipid monolayers and the conformations induced by the lipid environment. Synthetic signal peptides from E. coli outer membrane protein insert spontaneously into monolayers of mixed phosphatidyl ethanolamine/phosphatidyl glycerol (palmitoyl and oleoyl acyl chains). We have transferred the resulting peptide/lipid monolayers onto quartz plates or germanium crystals at a constant film pressure. Circular dichroism (CD) spectra of the peptide/lipid monolayers on quartz plates show increased α-helix content for the peptides inserted into the lipid phase relative to aqueous signal peptides, and adoption of a β-like conformation by the signal peptides adsorbed to the lipid surface (not inserted). FT-IR spectra obtained by attenuated total reflectance spectroscopy of the peptide/lipid monolayers on germanium crystals confirm both the helical tendency of the inserted signal peptides and the enhanced β-structure in the surface-adsorbed peptide. These observations are consistent with a model of the initial signal sequence/membrane encounter that involves conformational change first to a β-structure, as the signal peptide interacts with the membrane surface, then to α-helix as it inserts. These steps may facilitate the orientation and initial insertion of the mature protein.

T-AM-C12 Depolymerization of Microtubules Alters Plasma Membrane Potential and the Motional Freedom of ESR Probes in the Membrane. A. ASZALOS, S. DAMJANOVICH and M. M. GOTTESMAN. Division of Drug Biology, Food and Drug Administration, Washington, D.C. Department of Biophysics, Medical School of Debrecen, Debrecen, Hungary and National Cancer Institute, National Institutes of Health, Bethesda, MD. (Introduced by A. SZABO).

In the course of studing effects of microtubule depolymerizing drugs, three lines of evidence were obtained indicating that microtubule depolymerization affects the function and the physical state of the plasma membrane. One line of evidence was obtained with a membrane potential sensing dye and flow cytometry. Microtubule depolymerization with vincristine, (2.5 ug/ml) Colcemid, (0.5 ug/ml) and colchicine, (2.5 ug/ml) resulted in membrane depolarization in Chinese hamester ovary cells. These effects were due to drug interaction with microtubules because 1) effects were time dependent, 2) required the entry of the drugs into the cell as indicated by the lack of membrane depolarization in a multi-drug resistent mutant, 3) Colcemid-resistent tubuline mutant did not show membrane potential changes and 4) taxol, the microtubule stabilyzing drug, prevented the action of the depolymerizing drugs. Similar conclusions could be drawn from ESR studies using maleimid spin probes attached to proteins in the membrane. The third line of evidence comes from ESR probing the lipid domain of plasma membranes. These studies indicate that the motional freedom of the probes, as expressed by the order parameter S is higher in microtubule depolymerized cell membranes than those of untreated cells. Our finding indicate that microtubule affecting drugs influence the function of cells via changes in plasma membrane funtctions.

T-AM-C13 MEMBRANE-SPANNING REGIONS OF INTEGRAL MEMBRANE PROTEINS. C. M. Deber, C. J. Brandl, R. B. Deber, L. C. Hsu, and X. K. Young, *Research Institute, Hospital for Sick Children, Toronto M5G 1X8; and Departments of Biochemistry, Banting and Best Medical Research, and Community Health, University of Toronto, Toronto M5S 1A8, Ontario, Canada.*

Molecular mechanisms by which integral membrane proteins transport substrates across cellular membranes remain uncharacterized in many systems. We propose that specific membrane-located residues of the transport protein must confer appropriate specificities and provide the interactive forces which facilitate the movement of a hydrophilic substrate through the nonpolar midsection of the membrane. To identify these potentially functional amino acids, we have assembled the available sequence data for aqueous and intramembranous regions of integral membrane proteins, divided the proteins into transport (T) and non-transport (NT) categories, and analyzed the resulting data set (10,000 amino acids in 24 integral membrane proteins - 10 T and 14 NT proteins) for amino acid composition of membrane (M) and aqueous (A) domains. A-domains were largely identical between protein categories. However, M-domains of T proteins (but not of NT proteins) were characterized by the (statistically significant) selective inclusion of three amino acids: Pro, Asn, and Tyr. These residues are discussed in terms of their ability to participate in substrate interaction during transport. In addition, this analysis supports the hypothesis of Brandl and Deber (*Proc. Natl. Acad. Sci. U.S.A.*, 83, 0000 (1986), *in press*) that local structural changes arising from the regulated cis-trans isomerization of membrane-buried X-Pro peptide bonds in T proteins could realign membrane-spanning amphipathic helices to create a substrate-accessible pore.

T-AM-D1 INSULATION OF THE CONDUCTION PATHWAY OF MUSCLE TRANSVERSE TUBULE CALCIUM CHANNELS FROM THE SURFACE CHARGE OF BILAYER PHOSPHOLIPID. Roberto Coronado and Hubert Affolter. Department of Pharmacology, University of North Carolina, Chapel Hill, NC 27514.

Functional calcium channels present in purified rat muscle t-tubules (BJ 48:341, 1985) were inserted into planar phospholipid bilayers composed of the neutral lipid phosphatidylethanolamine (PE), the negatively charged lipid phosphatidylserine (PS), and mixtures of both. Barium current carried through the channel saturates as a function of bulk activity at a maximun conductance of 20 pS and a half saturation of 20 mM. Inward and outward currents, measured above and below the half saturation, were independent of bilayer mole fraction of PS from X_{PS}=0 (pure PE) to X_{PS}=1 (pure PS). In the absence of divalent ions it is shown that calcium channels transport sodium or potassium ions (P_{Na}/P_K=1.4) at saturation rates higher than those for divalent cations alone. In pure PE bilayers, sodium conductance saturates as a function of bulk activity according to a rectangular hyperbola with a half saturation of 0.2 M and a maximun conductance of 68 pS. Sodium conductance in pure PS bilayes is higher than in pure PE bilayers at activities below 0.1 M (1.8 fold at 48 mM). The maximun channel conductance at high ionic strength is unaffected by lipid charge. This modest difference at low ionic strength is well fitted by the Bell and Miller electrostatic equations (BJ 45:279, 1984) as if the conduction pathway of the calcium channel protrudes from the plane of the bilayer polar groups by a distance >20 Angstroms. This distance thereby effectively insulates the ion entryway to the channel from the lipid surface charge. Current versus voltage curves in pure PE and pure PS shows that the same conduction insulation is present on both ends of the calcium channel. Supported by NIH grant R01 GM 32824.

T-AM-D2 THE SIDEDNESS OF RECONSTITUTED CALCIUM CHANNELS FROM MUSCLE TRANSVERSE TUBULES AS DETERMINED BY D600 AND D890 BLOCKADE. Hubert Affolter and Roberto Coronado, Department of Pharmacology, University of North Carolina, Chapel Hill, NC 27514.

The verapamil-type calcium channel blocker, D600, and its charged quaternary derivative D890, were used to assess the sidedness of blockade in single calcium channels reconstituted from purified t-tubules. Spontaneous single channel openings were induced with the agonist Bay-K8644 and recordings were made in a two-chamber planar bilayer setup so that drugs could be deivered to either side of the channel (Affolter and Coronado, Biophys. J. 48:341-347, 1985). Micromolar drug addition resulted in a >10 fold decrease in probability of open channel events (p_o) without a significant change in single channel current amplitude. Changes in p_o occurred in paralel with changes in mean open time and both parameters could be titrated with similar IC_{50}. At pH 7.2, cis or trans D600 blocked with an IC_{50} of 5μM but for D890, the IC_{50} was cis 3μM and trans >75 μM. These results confirm that reconstituted t-tubule calcium channels insert into planar bilayers with the cytoplasmic end on the cis chamber, as previously argued on the basis that p_o increases with cis-positive potentials. The asymmetry of D890 blockade indicates that the drug can readily gain access to the blocking site from the aqueous solution adjacent to the inner but not extracellular end of the channel. The fact that cis D600 and cis D890 inhibit with similar IC_{50}'s strongly suggests that in both cases the cationic form is pharmacologically active. The kinetics of D890 blockade are consistent with an OPEN·DRUG → BLOCKED type of action with exceedingly long blocked times. Supported by a fellowship from Swiss National Funds and by NIH grant R01 GM 32824.

T-AM-D3 EFFECT OF ADRENALINE ON TWITCH TENSION AND ON SLOW CALCIUM CHANNELS FROM FROG SKELETAL MUSCLE. J. Arreola, J. Calvo, M.C. García and J.A. Sánchez. Dept. of Pharmacology, CINVESTAV, IPN and Biophysics, ENCB, IPN, Mexico City.

Catecholamines potentiate twitch tension possibly via AMPc (J. Physiol. 315: 267-282). The present experiments analyze the role of extracellular Ca^{2+}. Results are expressed as mean ± S.E. (n). T=20-22°C.

Mechanical experiments.- Single muscle fibers from Rana pipiens were used. Adrenaline (10^{-6}-10^{-5} M) increased maximum twitch tension (118% ± 11% (6)) in standard Ringer, and the effect was maintained throughout the experiments (ca. 30'). In low Ca^{2+} ($CaCl_2$ replaced by 3 mM $MgCl_2$), tension was also increased (119% (2)), but reversibly decreased down to ca. 77% at 14'.

Electrophysiological experiments.- Intracellular calcium action potentials from sartorius muscles were recorded. Control solution (mM): Na_2SO_4=80, TEA_2SO_4=40, K_2SO_4=2.5, $CaSO_4$=9, sucrose=460; pH= 7.2 (MOPS). Resting potential was -80.7 ± 0.6 (21) mV and with Adrenaline (10^{-5}M) added was -82.6 ± 0.7 (42) mV. $(dE/dt)_{max}$ (mV/s) were 145.0 ± 12.8 (21) and 267.7 ± 21.7 (42), respectively. Vaseline gap voltage clamp experiments on cut fibers were performed. External solution contained 10 mM Ca^{2+}, TEA=108 and methanesulphonate as anion. Control internal solutions (mM): TEA_2EGTA=75, Na_2ATP=3, DTT=2.5, pH=7.1. Peak calcium currents (I_{Ca}), decreased to 30% (2) in ca. 100'-110'. Addition of catalytic subunit of AMPc dependent protein kinase (10μg/500μl) to the E pool increased I_{Ca} by 50% (2) after correction for rundown. Twitch potentiation by Adrenaline does not require external Ca^{2+} in the short term, though a possible role for longer times is suggested, which might be mediated through calcium channels.

Partially supported by CONACyT grant PCCBBNA-022593.

T-AM-D4 GLUCOSE RESPONSE TO BURSTING-SPIKING PANCREATIC β-CELLS. Teresa Ree Chay, Department of Biological Sciences, University of Pittsburgh, Pittsburgh, PA 15260.

A mathematical model of the pancreatic β-cell electrical activity was developed using a barrier kinetic model. Our model incorpolates the glucose sensitive channel which is known to conduct K^+ in the absence of glucose. The model also incorporates Ca_i-sensitive K^+ channels which are inhibited by intracellular H^+ ions. It is described by three non-linear simultaneous differential equations. Numerical integration of these euqations allowed us to examine the effect of glucose and of external Ca^{2+} and K^+ ions on the electrical and cellular activity of the β-cell. Our results show that the contribution of glucose-sensitive channel activity, if not completely inhibited, plays a very important role in determining the bursting periodicity. Our results also shows that even a small decrease in pH_i is sufficient to change a bursting β-cell to a spiking one. The rich transient electrical activity, which occurs a few minutes after an addition of glucose, can be explained from our model by incorporating the intracellular acidification due to the mitochondrial sequestration.

* This work was supported by NSF PCM82 15583.

T-AM-D5 GLUCOSE-INDUCED OSCILLATORY CHANGES IN EXTRACELLULAR IONIZED CALCIUM CONCENTRATION IN MOUSE ISLETS OF LANGERHANS. Elia Perez-Armendariz, Illani Atwater & Eduardo Rojas, LCB & G, NIH Bethesda, MD. 20205.

Liquid membrane (Ca^{2+})-sensitive microelectrodes (1 μm tip diameter) were used to measure changes in the intercellular ionized calcium concentration in mouse pancreatic islets of Langerhans. Simultaneous recording of membrane potential from one B-cell and (Ca^{2+}) inside the same islet showed oscillations in calcium concentration in phase with the oscillatory bursts of spike activity. The calcium concentration in the intercellular space decreased during the active phase of the bursts of glucose-induced electrical activity (mean amplitude 0.58 ± 0.13, n=5 with the microelectrode tip at a mean depth of 60 μm). Minimum concentration in the intercellular space was reached near the end of the active phase of the bursts, showing that the temporal course of Ca^{2+} depletion was the mirror image of the cyclic K^+ acummulation reported in the same preparation previously (1).

If one considers that the brief burst of Ca^{2+} action potentials represents a sudden Ca^{2+} unloading of the intercellular space, then from the initial rate of depletion of Ca^{2+}, the calcium entry per unit area of B-cell membrane per action potential was calculated as 0.5 pmol/ cm^2s. Taking the B-cell membrane area as 500 X 10^{-8} cm^2 and a mean spike frequency of 5 s^{-1} one gets about 0.5 X 10^{-18} mol entering the B cell per spike.

(1) Elia Perez-Armendariz, Illani Atwater & Eduardo Rojas, Biophysical Journal Vol. 48 Nov. 1985.

T-AM-D6 GLUCOSE MODULATION OF CYTOSOLIC CALCIUM BUFFERING IN THE PANCREATIC B-CELL AS REFLECTED BY THE INSULIN RELEASE PATTERN IN RESPONSE TO K^+-INDUCED DEPOLARIZATION.
Susanne Joost and Illani Atwater, LCB & G, NIH, Bethesda, MD 20205.

Glucose-induced insulin release is known to depend on Ca^{2+} entry through voltage-gated Ca^{2+}-channels. Ca^{2+}-channel activation is inhibited by increased cytosolic Ca^{2+}. Thus, secretion may be expected to reflect Ca^{2+}-channel activity, the release process being activated by very localized, transient, increases in cytosolic Ca^{2+}, and Ca^{2+}-channel activity may be expected to reflect a more generalized cytosolic Ca^{2+} accumulation. In the experiments reported here, single large microdissected mouse islets of Langerhans were used. Membrane potential and insulin release were measured in response to 50 mM K^+-induced depolarization, applied in the presence of various glucose concentrations. In the absence of glucose, peak insulin release was 85% of the peak release in the presence of 5.6 mM glucose; in both conditions, peak release occurred about 1 min after the onset of depolarization. The ensuing time-course of the release, however, was very different. In the absence of glucose, K^+-induced release fell to a steady-state level about 30% of the peak value with a time constant of 9.4 min. In the presence of 5.6 mM glucose, the steady-state K^+-induced release was 84% that of the peak value and the time course for the decay in release was greater than 30 min. It may be concluded that the slow decay in release is due to secretion processes occurring after Ca^{2+} entry. Furthermore, insulin release may reflect inactivation of the Ca^{2+}-channel and in turn may indicate the time course and level of accumulation of Ca^{2+} in the B-cell cytosol.

T-AM-D7 VOLTAGE-GATED INWARD CURRENTS IN PANCREATIC ISLET B-CELLS. L.S. Satin and D.L. Cook, Depts. of Physiology and Biophysics, and Medicine, Univ. of Washington and VA Medical Center, Seattle, WA 98108.

Periodic bursts of Ca spikes, induced by glucose, mediate the Ca uptake necessary for sustained insulin secretion. In order to study the underlying ionic currents, we voltage-clamped cultured neonatal rat B-cells using a whole-cell patch clamp. Outward K+ channels were suppressed by replacing KCl with CsCl in EGTA- and HEPES-buffered pipette solutions, while 10mM TEA was added to HEPES-buffered bath solutions. Ba++ (3mM) was used as a Ca++ analogue to enhance inward current. Depolarizing voltage commands (40msec) from a holding potential of -50mV beyond a threshold voltage ($\sim$ -40mV) elicited inward current. The inward current peaked (<60pA) between -20 and 0mV, did not inactivate significantly within 40msec and became outward between +20 and +70mV. Replacement of Ba++ by Ca++ reduced inward current amplitude. Current was abolished by removing Ba++ (replaced by Mg++) or by adding the Ca++ channel blockers Co++ or Ni++ (2mM). The Ca++ channel agonist BAY K 8644 (5μM) reversibly increased the current.

Depolarizing commands from holding potentials $\geq$ -80mV elicited rapidly activating and inactivating transient inward currents in addition to the slowly inactivating Ba++ current. The largest transient component was blocked by Na+ removal (replaced with choline) or by the inclusion of 3μM TTX. We conclude that the B-cell membrane contains both Na+ and Ca++ channels. These membrane currents may contribute to the pattern of electrical activity exhibited by B-cells.

L.Satin was supported by NIH NS07097 and the Diabetes Research Council of Seattle; D.Cook by NIH AM29816 and the Veterans Administration

T-AM-D8 **A VERY SLOW CURRENT IN VENTRICULAR CELL**

KS Lee, JP Hansen, EW Lee - The Upjohn Company, Kalamazoo, MI.

The possible existence of a very slow Ca current of the ventricular cells (Lee et al 1984) was examined in this study using the suction pipette internal perfusion method. In external solution containing (mM) 150 Na, 5 Ca, 1 Mg, 0.01 TTX, 1 Cd, 1 Cs, 5 TEA and internal solution containing 150 Cs with 5 TEA and 10 EGTA, a very slow time and voltage dependent inward current is obtained. Activation time constants range from 400 msec at threshold potential of -70mV to about 200 msec at +30 mV. Peak whole cell inward current is less than 1 nA at -30 mV, becoming zero at 0 to +10 mV. Above this potential, an outward current is observed. A series of tests designed to establish a reversal potential indicated that the outward current which is carried by Cs moves through the same channel with a definable reversal potential. In Ca containing sodium free external solution, this channel carries a small inward Ca current whose size depends on external Ca concentrations. This inward current becomes significantly larger if Na is added to the Ca containing solution. However, if Ca is removed from the external solution in the absence or presence of 150 mM Na, both the inward and the outward current disappear completely, leaving a time independent leakage current. Reduction of external Na moves reversal potential to more positive levels. The current is not affected by high doses of verapamil but is enhanced by low doses of epinephrine. Current clamp studies showed that this current generates a Cd insensitive slow action potential similar to that reported by Lee et al earlier.

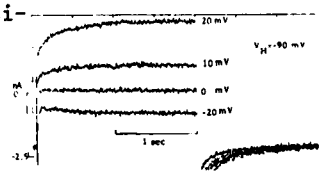

Ref: KSLee,DNoble,ELee & AJSpindler(1984) Proc. R. Soc. Lond. B223:35-48

T-AM-D9 AEQUORIN GLOW IN SQUID AXONS AS INFLUENCED BY MEMBRANE POTENTIAL. J. Requena, J. Whittembury*, & L.J. Mullins, Centro de Biociencias, Instituto Internacional de Estudios Avanzados, Caracas 1011, Venezuela, Department of Biochemistry & Biophysics, University of Pennsylvania, Philadelphia, PA, Department of Biophysics, University of Maryland School of Medicine, Baltimore, MD 21201.

Squid giant axons were kept in a solution that was 150 mM each of Na, K, and Tris together with TTX, 3,4 diamino Pyridine, 50 mM Mg and 3 mM Ca. In such a solution, membrane potential was about -10 mV and this potential could be altered by voltage clamp. In an aequorin-injected axon, a steady hyperpolarization reduced aequorin glow and caused an alkaline shift in pH_i as measured with a glass electrode. Steady depolarization increased light emission and caused an acidification of the fiber. Voltage clamp pulses produced similar but smaller effects on aequorin light emission. If the solution bathing the axon was made Ca-free, steady hyperpolarization still reduced aequorin light emission but depolarization either of a steady sort or with pulses had a smaller effect suggesting that Ca efflux is controlling the level of $[Ca]_i$ (there is no influx since Ca_o is zero). If large depolarizing pulses were applied (+150 mV pulse amplitude) at a duration of 5 msec, the response was larger than if a pulse of half the amplitude and twice the duration. Hyperpolarizing pulses decreased resting aequorin glow, and a pulse protocol where pulses of identical amplitude and duration but alternating in sign (i.e. a depolarizing pulse was followed by a hyperpolarizing pulse) produced little or no change in aequorin light output.

This work was aided by the National Institutes of Health (1 R01 NS17718), the National Science Foundation (BNS 8006271), and the Consejo Nacional de Investigaciones Cientificas (S1-1198).

T-AM-D10 VERAPAMIL SENSITIVE CALCIUM CHANNELS ASSOCIATED WITH EXOCYTOSIS IN PARAMECIUM. Alice L. Vuoso and Birgit H. Satir (Intr. by J. Condeelis), Department of Anatomy and Structural Biology, Albert Einstein College of Medicine, Bronx, New York.

The effect of the calcium channel blocker verapamil on exocytosis of trichocyst matrices (tmx'es) in Paramecium tetraurelia was examined to study the possible role of calcium channels in this cell. Axenic cultures of Paramecium cells were harvested in log phase (3 days) and resuspended in PIPES buffer pH 7. Stimulation of exocytosis was induced with trinitrophenol (TNP), and the release response was scored according to number of tmx'es released per cell. Exocytosis in these cells has been shown to be calcium dependent and replacement of extracellular calcium with magnesium (20mM) inhibits TNP induced release. Addition of calcium (0.5mM) to this solution restores the ability of the cells to secrete. The secretory response of cells incubated in the presence of verapamil (30μM) is inhibited within ten minutes. An intermediate stage of release is obtained in which the cells are observed to secrete from the anterior and not the posterior portion of the cell body. The inhibitory effect of verapamil is reversible upon dilution with PIPES buffer. This study provides the first evidence for the involvement of calcium channels in exocytosis in Paramecium. In addition, it suggests the presence of either a gradient of calcium channels in the plasma membrane of these cells or a differential sensitivity of the calcium channels to verapamil.
This work was supported by grants from NIH and NCI.

T-AM-D11 DIFFERENT CALCIUM CHANNELS MEDIATE NEUROTRANSMITTER RELEASE FROM SENSORY AND SYMPATHETIC NEURONES. Teresa M. Perney, Lane D. Hirning and Richard J. Miller. Dept. of Pharmacological and Physiological Sciences, Univ. of Chicago, 947 E. 58th Street, Chicago, IL 60637, U.S.A. (Intr. by M.L. Villereal).

We examined neurotransmitter release evoked by depolarization from primary cultures of sympathetic neurones (superior cervical ganglia) and sensory neurones (dorsal root ganglia, DRG) isolated simultaneously from 1-2 day old rats. Raising the external $[K^+]$ induced the release of substance P from DRG neurones. This release could be blocked by Co^{2+} or in Ca^{2+} free medium. Release could also be evoked by Ba^{2+}, capsaicin or A23187. 70 mM K^+ induced release was considerably enhanced by the dihydropyridine (DHP) Ca^{2+} channel agonist, BAY K8644 over the concentration range 10^{-9}-10^{-6}M. The effects of 70 mM K^+ or a combination of 70 mM K^+ and BAY K8644 (10^{-6} M) could be blocked by the DHP antagonists nitrendipine and nimodipine or D-600 at low concentrations (< 10^{-6} M). Moreover, evoked substance P release was also enhanced by the DHP (+)-202791 and blocked by its enantiomer (-)-202791. Cultures of DRG cells possessed high affinity binding sites for ^{3}H-nitrendipine. In addition, we observed that a DRG x neuroblastoma cell line, F11, contained DHP sensitive Ca^{2+}-channels. Evoked release of substance P from this cell line was also increased by BAY K8644 and blocked by nimodipine. Cultures of sympathetic neurones released ^{3}H-norepinephrine upon stimulation with 70 mM K^+. Release was blocked by Co^{2+} or in Ca^{2+} free medium. In this case, however, DHP Ca^{2+} channel agonists or antagonists had no effect on release at concentrations up to 10^{-5} M. D-600 caused some inhibition or release (approx. 40%) at high concentrations (10^{-5} M). Thus, DRG cells seem to utilize DHP sensitive Ca^{2+} channels to mediate transmitter release whereas sympathetic neurones do not. (Supported by PHS Grants DA-02121, 02575 and MH-40165).

T-AM-D12 ETHANOL INDUCES CALCIUM DEPENDENT CORTICAL GRANULE DISCHARGE, BLOCKS FERTILIZATION, AND INTERFERES WITH MITOSIS AND EMBRYONIC DEVELOPMENT IN SAND DOLLARS, Echinaracnius parma. Robert B. Silver[1,2] and Harrish C. Pant[3,2], [1]Laboratory of Molecular Biology, Univ. of Wisc., Madison, [2]Marine Biological Laboratory, Woods Hole, MA., [3]Lab. of Preclin. Studies, NIAAA, Rockville,MD.

Chronic human consumption of ethanol (EtOH) is associated with increased incidence of infertility, non-familial birth defects and fetal alcohol syndrome. Relevant cellular systems effected by EtOH, and the molecular mechanisms involved have yet to be identified. In order to determine the EtOH related effects on eggs, fertilization, mitosis and embryonic development eggs and embryos of the sand dollar, Echinaracnius parma, were treated with 0→100 mM EtOH. Microinjection of EtOH (10→100 pl) into single eggs (600 nl), in normal sea water (nSW) induced cortical granule breakdown (CG-BD), elevation of the fertilization envelope (FE-↑), cytoplasmic gelation and formation of a villus at the site of injection. EtOH injections in calcium free sea water did not induce CG-BD or FE-↑ (both dependent on external calcium in control cells), but did cause cytoplasmic gelation and formation of a villus at the site of injection. Villi retracted to the cytoplasm with time. Eggs bathed in nSW containing 30→50 mM EtOH exhibited partial or full CG-BD, and single or multiple site FE-↑. Above 50 mM there was complete CG-BD and full FE-↑. Eggs fertilized in nSW following chronic (1 or 7) hr. EtOH exposure showed concentration dependent effects: > 10 mM interfered with fertilization, > 30 mM caused irregular or incomplete mitoses, and > 50 mM frequently blocked fertilization. Embryos from eggs first fertilized in nSW, then transferred to to EtOH-nSW showed results similar to those described for eggs fertilized in > 30 mM EtOH-nSW. Embryos exposed to > 30 mM EtOH developed abnormally, with elongations of cellcycles related to EtOH concentrations. EtOH appears to exert its effects through calcium fluxes across both plasma- and endo-membranes.

T-AM-E1 SERIES RESISTANCE IS A MODULATED ELECTRICAL PROPERTY OF CRAYFISH GIANT AXONS. Sami Hassan and E. M. Lieberman. Dept. of Biology and Dept. of Physiology, Sch. Med., East Carolina Univ., Greenville, NC 27834.

Series resistance (R_S) of axons, which has been generally considered a constant, was found to vary with conditions known to effect the physiology of the adaxonal glia. R_S was estimated from computer analyzed voltage waveforms generated by standard current clamp and axial wire methods. The average R_S for crayfish giant axons in control conditions was 6.50 ± 0.50 ohm-cm^2. R_S increased up to 25% when the axon was stimulated at greater than 30 Hz. Carbachol (10^{-7}M) decreased and d-tubocurare (d-TC) (10^{-8}M) enhanced the R_S change caused by stimulation. High frequency stimulation or carbachol also cause hyperpolarization of the adaxonal glia while d-TC prevents the hyperpolarization. To evaluate the physiological role of the R_S changes Na depletion/replenishment kinetics (Tris or sucrose substituted) were studied using the AP overshoot as a measure of adaxonal [Na]. No change in AP overshoot occured with a 25% or less reduction in $[Na]_o$, but the R_S increased, on average, by 85% (range, 30 to 300%). With greater Na depletion the AP overshoot decreased in a Nernstian manner; there was no further increase in the R_S. The rate constant for Na_o depletion and replenishment were not different. After carbachol treatment R_S did not increase with Na depletion and Na depletion proceeds at a much increased rate as compared to replenishment.

The data suggest that, *in vivo*, the modulation of R_S by Na_o tends to conserve Na_o and cholinergic agonists speed replenishment under conditions of Na depletion (high frequency stimulation). The data can be correlated with changes in glial cell physiology and indicate a role in perineural ion homeostasis. Supported by ARO DAAG29-82-K-0182 and NSF INT 8117183.

T-AM-E2 THE EFFECT OF OUABAIN AND HEPTANOL ON INTRACELLULAR FREE CALCIUM IN THE RABBIT INTERATRIAL SEPTUM.

Lynn M. Crespo and Jose Jalife, Department of Pharmacology, State University of New York, Upstate Medical Center, Syracuse, New York 13210

Various compounds, including the cardiac glycosides and long chain alcohols, are known to induce electrical uncoupling of cardiac cells through changes in gap junction permeability. Calcium, pH and voltage have all been implicated in the regulation of gap junction permeability, but it is unclear what role each factor plays, since changes in one parameter may induce concomitant changes in the other. Measurement of intracellular free calcium, Ca_i, with the fluorescent Ca indicator Fura 2 demonstrated that 5 x 10^{-8} to 1 x 10^{-5} M ouabain reversibly increased the mean Ca_i in the rabbit interatrial septum from 78 ± 18 nM (n=10) by a variable amount of 5-60 nM in 2 hours. The amount of Ca gained was independent of ouabain concentration. Decreasing Na_o from 140 to 90 mM, a condition which inhibits ouabain-induced uncoupling, elevated mean Ca_i to 153 ± 18 nM (n=4). Exposure of the tissue to 1 μM of the Ca ionophore A23187 in the presence of 1.8 mM Ca rapidly increased Ca_i to > 10 μM. Subsequent addition of 5 mM EGTA then decreased Ca_i to < 1 nM, demonstrating that Fura 2 is responding to changes in Ca_i. Heptanol, which also blocks junctional conductance and promotes electrical uncoupling, did not affect Ca_i when used at concentrations up to 3 mM (n=4). These observations suggest that elevated Ca_i is not responsible for the decreased gap junction permeability and electrical uncoupling of cardiac cells in response to these compounds.

T-AM-E3 DIFFERENTIAL CLOSURE OF mRNA-INDUCED AS COMPARED TO ENDOGENOUS CELL-CELL CHANNELS IN PAIRS OF XENOPUS OOCYTES. G.P. Dahl and R. Werner, Depts. of Physiology & Biophysics and of Biochemistry, University of Miami, Fl. 33101.

Microinjection into Xenopus oocytes of mRNA isolated from estrogen-stimulated rat myometrium results in the induction of cell-cell channels between paired oocytes (Werner et al., J. Membrane Biol. 1985). mRNA-induced channels can be observed against a zero background or as an easily discernible increase over a low level of endogenous channels depending on the maturation state of the oocytes.

Junctional conductance was determined by dual voltage clamp in mRNA-injected pairs of oocytes and in control pairs with endogenous channels. The pairs were subjected to several uncoupling procedures: intracellular concentrations of H^+ or Ca^{2+} were modified by injection of buffer solutions close to the junction or a transjunctional voltage gradient was established.

Endogenous oocyte-oocyte channels were found to be: (i) pH sensitive; the channels close when buffers with a pH as high as 6.8 are injected, (ii) sensitive to transjunctional voltage which reduces conductance symmetrically across the junction, but (iii) insensitive to $[Ca^{2+}]$ of 10^{-4} M.

In contrast, oocyte-oocyte channels induced by mRNA are: (i) closed by 10^{-5} M $[Ca^{2+}]$, (ii) less sensitive to pH changes (pH < 6.5), and (iii) insensitive to transjunctional voltage.

These data indicate that mRNA-injection into oocytes induces cell-cell channels which are qualitatively different from endogenous channels. mRNA isolated from rat heart induces channels with the same characteristics as generated by myometrial mRNA. Supported by NSF (PCM8216153).

T-AM-E4 **MODULATION OF ELECTRICAL COUPLING BETWEEN CELLS OF THE LENS.** R.T. Mathias and J.L. Rae, Depts. of Physiology & Biophysics, SUNY Stony Brook, NY and Rush Med Col, Chicago, IL.

We have studied a number of substances which modulate coupling in the intact frog lens. Two intracellular microelectrodes are placed within the lens, one near the center to pass current and the other at various depths to record the induced voltage. When the injected current is a high frequency sinusoid, the surface membrane capacitance poses little impedance, hence the induced potential is primarily due to the resistance of those junctions between the point of recording and the bath. We use this technique to record either time dependence or spatial dependence of junctional resistance.

The general conclusions are: 1) Junctions near the lens surface are quite sensitive to pH. Bubbling with 100% CO_2 causes a reversible increase in junctional resistance of at least 20 fold; this effect is complete in approximately 30 minutes. 2) The pH sensitivity declines as one moves into the lens and cells located interior to 75% of the radius do not uncouple, at least for up to 12 hours in 100% CO_2. 3) Outer cells will uncouple in response to elevated intracellular Ca but we could induce only about a 2 fold increase in junctional resistance; we did not attempt to characterize the radial dependence of this relatively small change. In 20 mM bath Ca the effect required 12 hours whereas addition of the ionophore A23187 reduced the time to 5 hours. 4) Other agents, which are likely to affect intracellular Ca or pH, will modulate cell to cell coupling. For example: soaking in 100 μM ouabain causes a slow steady uncoupling; replacing bath chloride with propionate causes a more rapid, reversible uncoupling. (Supported by NIH grants EY03095 and EY03282).

T-AM-E5 **THE DYNAMICS OF SIGNAL TRANSFER BETWEEN RODS AND BIPOLAR CELLS IN THE VERTEBRATE RETINA** **M. Capovilla, W. A. Hare, W. G. Owen & A. Wang. Dept. of Biophysics & Medical Physics, University of California, Berkeley.**

Linear range responses, elicited by dim, 20 msec flashes of 500 nm light, were recorded intracellularly from rods and bipolar cells in the isolated, perfused retina of the larval tiger salamander, Ambystoma tigrinum. Cells were identified on the basis of their response properties which earlier had been correlated with cell type by injection of HRP and subsequent histological study. Stimuli were spots of light, 600 um in diameter, centered within the cells` receptive fields. Responses were well-fitted by arbitrary linear functions scaled in proportion to stimulus intensity. Taking the Fourier transforms of these functions, we calculated the transfer function of the rod/bipolar cell "synapse". The amplitude transfer function, (gain), was bandpass in form, with a maximum near 2 Hz and a steep roll-off at frequencies above 5 Hz. The synapse introduced phase lead at frequencies below about 3 Hz and phase lag at higher frequencies. It thus behaves as a tuned filter; but tuned to what?

The rod network exhibits high-pass filtering properties, the network length constant being short at frequencies below 0.5 Hz and rising to a maximum value at 1 - 2 Hz. The synapse is therefore tuned to those components of the rod response that have the widest spatial distribution, transmitting them to the bipolar cell with maximum gain and zero delay. Hence, a significant spatial processing of the bipolar cell's input is due to the temporal filtering properties of the synapse. (Supported by NIH research grant #EY03875 to W.G.O.).

T-AM-E6 THE PRINCIPAL GAP JUNCTION POLYPEPTIDE IS A PHOSPHOPROTEIN: ITS PHOSPHORYLATION AND JUNCTIONAL CONDUCTANCE ARE STIMULATED BY cAMP. J.C. Saez, D.C. Spray, +E.L. Hertzberg, *A.C. Nairn, *P. Greengard, and M.V.L. Bennett, Albert Einstein College of Medicine, N.Y. +Baylor College of Medicine, Houston, Texas and *Rockefeller University, N.Y.

Liver cells dissociated into small groups (prepared from adult rats by collagenase perfusion) were labeled with ^{32}P for 1 hr. The 27kDa major gap junction polypeptide was immunoprecipitated, 1 hr after the labeling period, from SDS solubilized cells using an antibody raised against liver gap junctions and protein A-bearing staphlococcus. Autoradiographs of the 12.5% SDS-PAGE used to resolve immunoprecipitated proteins show that 27kDa is phosphorylated: ^{32}P incorporation was about doubled when 8Br-cAMP (1 mM) was applied. The time course of ^{32}P incorporation with or without 8Br-cAMP was followed for 30 min. In the absence of the cyclic nucleotide, incorporation did not change: in its presence, ^{32}P incorporation was progressively increased. Phosphoamino acid analysis of the immunoprecipitated 27kDa phosphoprotein revealed that serine is the amino acid residue phosphorylated. These data are consistent with our previous report of cAMP dependent phosphorylation of isolated 27kDa (J. Cell Biol. abstr., in press) and is correlated with functional change: Membrane permeant cAMP derivatives increase gap junctional conductance (g_j) within minutes when applied to voltage clamped pairs of hepatocytes. Glucagon also increases g_j, an effect prevented by intracellular injection of the protein inhibitor of the cAMP dependent protein kinase (Walsh Inhibitor). Macroscopic increase in g_j could reflect phosphorylation of the 27kDa polypeptide through the cAMP dependent kinase: confirmation of direct action awaits the demonstration of phosphorylation effects in reconstituted systems.

T-AM-E7 COMPARISON OF GAP JUNCTIONAL CONDUCTANCE/PERMEABILITY RATIOS AMONG EARLY EMBRYONIC CELLS OF FROG, FISH AND SQUID. V. Verselis, D.C. Spray, R.L. White and M.V.L. Bennett, A. Einstein College of Medicine, Bronx, N.Y.

The ratio between gap junctional conductance (g_j) and permeability to tetra-alkylammonium ions (P_j(TAA)) was determined in isolated cell pairs from embryos of Rana (frog), Fundulus (fish) and Loligo (squid). Gap junctions of these tissues differ in sensitivity to voltage and pH and in apparent dye permeability, suggesting possible differences in effective channel size or permissiveness. P_j was determined by monitoring TAA flux from pre-injected to post-junctional cells with ion-selective electrodes (Biophys J. 47:504a, 1985). g_j was measured either directly by double voltage clamp or indirectly by applying the pi-tee transform to current clamp data. In fish and amphibian embryos, t-methyl (TMA), t-ethyl (TEA) and t-propylammonium (TPA) were permeable and the P_j/g_j ratios (1.5×10^{-3}, 8×10^{-4}, and 1×10^{-4} cm^3/sec/S, respectively) were constant over the g_j range 0.2-2.0 uS. P_j to tetrabutylammonium (TBA) was extremely low, consistent with slow and often undetectable transfer of fluorescent dye molecules similar in size. In preliminary analysis P_j/g_j ratios in squid for TMA and TEA are similar, although somewhat elevated relative to frog and fish. Transfer of TBA (and fluorescent dyes: Lucifer Yellow and fluorescein derivatives) was often evident, but may be due to the very high g_j in this preparation (>10 uS). Similar P_j/g_j ratios in these various preparations imply that channel size is constant despite the apparent differences in dye permissiveness and regulatory properties of these gap junction channels.

T-AM-E8 INTERCELLULAR ELECTROPHORESIS OF CHARGED MOLECULES THROUGH GAP JUNCTIONS BY EXTERNALLY APPLIED ELECTRIC FIELDS. Mark S. Cooper and John P. Miller, Department of Zoology, University of California, Berkeley, CA 94720.

An ensemble of cells connected electrotonically by gap junctions will react as a finite length, leaky cable to an external electric field. In a uniform DC field E, a membrane potential profile given by $V(x) = -E\lambda \sinh(x/\lambda)/\cosh(l/\lambda)$ is imposed on a linear chain of cells of length 2l, where λ is the electrical length constant of the cellular ensemble, and x is the distance from the geometric center of the chain. When the length of the ensemble exceeds λ, a large current from the external medium penetrates the cell membranes of the cellular ensemble and flows through the coupled cytoplasms. This current generates an electric field within the cytoplasms of the electrotonically coupled cells which is given by $E_{internal} = -(d/dx)(V + Ex) = E(1 - (\cosh(x/\lambda)/\cosh(l/\lambda)))$. Previously, it was suggested that this internal electric field could move charged cytoplasmic molecules through gap junctions by electrophoresis (Cooper, J. Theor. Biol. 111 (1984) 123). We have now established this electrophoretic movement between cells experimentally using the crayfish ventral nerve cord. Fluorescein was injected iontophoretically into lateral giant neurons within the third segment of the nerve cord. Subsequently, the nerve cord was exposed to a 2.5 V/cm field. Within 90 minutes, the bolus of injected fluorescein migrated through two sets of gap junctions and accumulated in the dendritic processes of the lateral giant in the terminal ganglion which faced the anode. Additional tissues in which the intercellular electrophoresis has been detected will be described. Application of controlling the distribution of small charged molecules within electrotonically coupled tissues by an externally applied electric field are also discussed.

T-AM-E9 GAP JUNCTIONS IN TUNICATE EMBRYOS: pH AND VOLTAGE GATING MECHANISMS J. Knier, V.Verselis D.C. Spray and M.V.L. Bennett (Intr. by E.B. Masurovsky). Albert Einstein College of Medicine, Bronx, New York, 10461.

Gap junctional conductance, g_j, in tunicate embryos is steeply and symmetrically reduced by transjunctional voltage, V_j, of either sign with sensitivity comparable to that in amphibian embryos (Knier and Bennett, Biol. Bull., 169:3, 1985, cf. Spray et al., J. Gen. Physiol. 77:77-93,1981). We examined pH dependence of g_j in embryos of the tunicate Ciona intestionalis. When dechorionated and placed in contact, fertilized (but not unfertilized) eggs became coupled within minutes. Separate current and voltage electrodes in each cell were used to measure g_j and nonjunctional conductances. An electrode filled with liquid ion exchange resin was used to determine cytoplasmic pH, pH_i. In artificial sea water at pH 7.6, pH_i was about 7.5. Bathing in CO_2 equilibrated sea water rapidly reduced g_j to very low levels, which recovered on rinsing in normal sea water. In one cell pair, the relation between g_j and pH_i was determined. g_j was reduced to half at a pH_i of about 6.8, but 5% still remained at pH_i 6.3. The relation was at least approximately the same during acidification and recovery. At low pH_i, g_j still retained voltage sensitivity, but more quantitative measurements are required to determine whether voltage dependence of the remaining g_j has the same parameters as the much larger g_j at normal pH_i (as is true of junctions in amphibian embryos). The voltage and pH gating mechanisms may be involved in compartment formation during normal development.

T-AM-E10 ANALYSIS OF GAP JUNCTION ELECTRON MICROGRAPHS BASED ON A THREE-DIMENSIONAL MODEL.
G. Sosinsky*, D.L.D. Caspar*, T.S. Baker**, L. Makowski†, S. Maulik††, W. Phillips* & D. Goodenough¶. *Rosenstiel Center, Brandeis University; **Dept. of Biological Sciences, Purdue University; †Dept. of Biochemistry, Columbia University; ††Biophysics Graduate Program, Brandeis University; ¶Dept. of Anatomy, Harvard University.

Starting with information about the structure of gap junction membranes from low-irradiation electron micrographs of negatively stained and frozen-hydrated specimens and from X-ray diffraction patterns of partially oriented hydrated specimens, a three-dimensional model of the connexon pair has been constructed at a resolution of about 20 Å. This model is being refined against the available EM and X-ray diffraction data. A distinctive aspect of the gap junction membrane structure problem is that the connexon domain at the cytoplasmic surface is very labile. X-ray diffraction and EM data from selected specimens we have analyzed provide self-consistent evidence for an ordered surface structure, but this order is frequently lost in specimens observed in the electron microscope. In the model based on data from well-ordered specimens, the cytoplasmic side of the connexon channel is closed by a prominent gate structure about 20 Å thick located about 60 Å from the middle of the gap; the connexon units are connected together in the hexagonal lattice by cytoplasmic domains joined at the three-fold axes which project out to about 90 Å from the middle of the gap; and there are hexagonally arrayed pits between the trigonal projections and the cap on the channel. Variation in the images from frozen-hydrated and tilted, negatively stained specimens can be accounted for by the degree of structural preservation of these labile cytoplasmic surface features.

T-AM-E11 GAP JUNCTION STRUCTURE: THE EFFECTS OF DETERGENT TREATMENT AND LATTICE VARIATION.
Edward Gogol and Nigel Unwin, Department of Cell Biology, Stanford University, Stanford, CA 94305

Significant differences, perhaps attributable to variations in sample preparation procedures, have been previously reported in investigations of gap junction structure by minimal-dose electron microscopy. To begin to understand these differences, and the relevance of these studies to the native state, we have examined the effects of the severity of treatment of specimens with the detergents used in their isolation. The primary effect of detergent treatment is a systematic contraction of the lattice dimension, from a maximum of about 90 Å to values as small as 79 Å, presumably by extraction of lipids from the junctional membranes. Accompanying the lattice shrinkage is a rearrangement of connexon packing, which can be described as an increasing deviation from p6mm symmetry. In projection maps from negatively stained images, this change shows up as an apparent rotation of the connexon with respect to the lattice. Based on the progressive nature of these changes, the native state of the gap junction seems best represented by those specimens with large lattice dimensions and p6mm packing symmetry (corresponding to p622 in three dimensions).

Supported by the Jane Coffin Childs Memorial Fund for Medical Research (E.G.) and NIH (N.U.).

T-AM-E12 STRUCTURE OF GAP JUNCTIONS: EVALUATION OF MOLECULAR MODELS BY DIRECT COMPARISON OF CALCULATED AND OBSERVED X-RAY DIFFRACTION PATTERNS
Lee Makowski Dept. of Biochemistry & Molecular Biophysics, Columbia University, 630 W. 168th St., New York, NY 10032

Gap junction structure is being studied by x-ray diffraction from partially oriented specimens. Intensities along lattice lines are extracted from diffraction patterns by angular deconvolution of the observed data and have been used for the construction of molecular models of the gap junction. Although intensities obtained in this way have proven reliable in application to several macromolecular assemblies, the deconvolution techniques used must necessarily amplify noise in the data; imperfect numerical representation of the background may lead to errors in the intensities; and the resolution of the resulting intensities is strictly limited. The most accurate data useful for testing a molecular model is not the derived intensities, but the unprocessed diffraction data. In order to use this data, methods have been developed and implemented for the point-by-point comparison of calculated and observed diffraction patterns. In this process, intensities calculated from the molecular model are multiplied by and convoluted with functions representing the disorder and disorientation within the specimen and corresponding to distortions due to beam size and camera geometry. Calculated and observed diffraction patterns can then be scaled and compared and residuals can be used to guide refinement of models. Quantitative evaluation of models for the gap junction structure are being made using this technique.

T-AM-F1 ELECTRON TRANSFER COMPONENTS OF MANGANESE-OXIDIZING BACTERIA. L.A. Graham, J.C. Salerno, H.L. Ehrlich, Biology Department, Rensselaer Polytechnic Institute, Troy, NY 12180

Bacteria isolated from the area of a deep sea hydrothermal vents of the Galapogos Rift (Mussel Bed vent) possess an inducible Mn^{2+}-oxidizing enzyme system. It has been previously demonstrated that the gram-negative strain SSW_{22} can couple ATP synthesis to manganese oxidation (Ehrlich 1983). Detergent fractionation of cell sonicates of SSW_{22} has resulted in the separation of electron transport chain components present in both the induced and uninduced systems. A cytochrome bc-type membrane complex was partially purified by centrifugation on a sucrose density gradient. Optical spectra of this fraction reveal a cytochrome c-type with α-maxima at 551 nm and 520 nm in addition to a cytochrome b-type peak at 563 nm. Analysis of the cytochrome bc-type complex fraction by Electron Paramagnetic Resonance produced spectra characteristic of low spin cytochromes with two absorbance peaks in the g=3.4 - 3.8 region suggesting two b-type cytochromes. A soluble c-type cytochrome with α-maximum at 550 nm and EPR g-value of ~ 3.4 was separated by hydroxyapatite chromatography. An EPR detectable nonheme iron protein with g values of 4.7, 4.0, and 4.6 was also present in the soluble fraction possibly having a role in Mn^{2+}-oxidation or electron transport.

T-AM-F2 EPR CHARACTERIZATION OF THE CYT D OXIDASE OF E. COLI AND THE EFFECTS OF SODIUM NITRITE. Steven W. Meinhardt, Robert B. Gennis*, and Tomoko Ohnishi, Department of Biochemistry and Biophysics, University of Pennsylvania, Philadelphia, PA 19104, *Department of Chemistry, University of Illinois, Urbana, IL 61801

The ubiquinol-cyt d oxidase found in E. coli has been shown to contain three spectroscopically distinct cytochromes; cyt d, cyt b_{595} (cyt a_1), and cyt b_{558} (1).We have studied this enzyme by EPR spectroscopy and have assigned EPR signals to each of the three cytochrome species by their redox behavior and pH dependence. Cyt d has been asigned to an axial high spin species, g = 5.95, and rhombic low spin species g=2.5, 2.3, E_{m7}=260 mV, 60 mV/pH unit. We have not as yet determined which of these species is the active form. Cytochrome b_{595} is a rhombic high spin species with g_z=6.3, g_y=5.7, E_{m7}=135 mV, 30 mV/pH unit. Cyt b_{558} is a low spin species with g_z=3.3, E_{m7}= 180 mV, 30 mV/pH unit. These results are consistent with the E_m values reported from optical titrations (2). When sodium nitrite is added to membrane particles at an E_h of -60 mV the g=6 signal titrated as two species with midpoints of approximately 220 and 350 mV, pH 8, and the g=6.3 signal of cyt b_{595} is split into two peaks at g=6.4 and g=6.2. In an optical titration the 630 nm peak of the reduced cyt d shifts to 640 nm and decreases in amplitude. The 640 nm peak titrated as two n=1 components with midpoints of 220 and 350 mV, pH 8, and were of approximately equal magnitude. Cytochromes b_{595} and b_{558} showed little or no effect apon addition of nitrite. (1) Koland, J.G., et al., Biochem, 23,1051-1056. (2) Lorence, R.M., et al.,Biochim. Biophys. Acta, 790, 148-153.

T-AM-F3 PROTON TRANSLOCATED TO ELECTRON TRANSFERRED RATIOS IN PHOSPHOLIPID VESICLES CONTAINING CONTROL, TRYPSIN-TREATED, AND SUBUNIT III-DEFICIENT BOVINE HEART MITOCHONDRIAL CYTOCHROME c OXIDASE. L.J. Prochaska, V.A. DiBiase and K.A. Reynolds, Biological Chemistry, Wright State University, Dayton, OH 45435.

Native gel electrophoresis [Ludwig et al., Biochemistry 18, 1401 (1979)] of bovine heart mitochondrial cytochrome c oxidase removes 85 to 95% of subunit III and most of components b and c (nomenclature of Capaldi) from the enzyme. This preparation has been reconstituted into asolectin phospholipid vesicles by cholate dialysis and these liposomes are impermeable to protons as assayed by the respiratory control ratio (RCR = 4.6 ± 1.2). Upon addition of ferrocytochrome c, liposomes containing 85% subunit III-deficient enzyme undergo an apparent proton translocated to electron transferred ratio (H+/e-) of 0.34 ± 0.15 (at one enzyme turnover, 4 e-/heme aa_3), whereas those containing 95% subunit III-deficient enzyme exhibit a H+/e- ratio of 0.05 ± 0.03. Trypsin-treatment of the enzyme results in the complete removal of component b and 85% of component c with partial cleavage of subunit IV and component a. Liposomes reconstituted with trypsin-treated enzyme have a RCR of 6.0 ± 0.9 and undergo a H+/e- of 0.79 ± 0.05 at one turnover of the enzyme. Liposomes containing control enzyme have a RCR value of 5.2 ± 1.4 and exhibit a H+/e- of 0.83 ± 0.06 at one enzyme turnover. 94 ± 6% of subunit III deficient enzyme, 89 ± 2% of trypsin-treated enzyme, and 95 ± 4% of control enzyme in the liposomes has been observed to have the cytochrome c binding domain toward the extravesicular medium as determined by cytochrome c oxidase reduction using impermeable (cytochrome c + ascorbate) and permeable (N,N,N',N'-tetramethyl-phenylenediamine) reductants. These results suggest that subunit III is responsible for 80-100% of the proton-pumping function of the enzyme and that components b and c have no role in maximum proton translocation activity. (NIH HL-29051).

T-AM-F4 NANOMOLAR QUANTITIES OF A SYNTHETIC POLYANION WILL INHIBIT THE MITOCHONDRIAL CHANNEL, VDAC. Choh L. Yeung, Joyce Tung, Marco Colombini and T. Konig*., Labs. of Cell Biology, Dept. of Zoology, Univ. of Maryland, College Park, MD 20742 and *Second Institute of Biochemistry, Semmelweis Univ. Med. School, 1088 Budapest, Hungary. (Intr. by Leonard Binstock)

A synthetic polyanion made by the copolymerization of methacrylate, maleate and styrene (1:2:3) had been previously shown (Konig et al., Biochim. Biophys. Acta 462: 380-389, 1977) to inhibit a variety of mitochondrial functions including State 3 respiration and ADP/ATP exchange. Here we present evidence that this substance inhibits the outer mitochondrial membrane channel, VDAC (isolated from N. crassa). Channels were inserted into planar phospholipid membranes and their properties studied prior to and following the addition of the polyanion. 50 ug/ml of polyanion will rapidly block virtually all channel conductance in 1 M KCl, 5 mM $CaCl_2$ solutions. However, as little as 30 ng/ml will reduce the conductance of VDAC-containing membranes. When VDAC channels are inserted into liposomes, and their ability to increase the liposomes' permeability to non-electrolytes is measured, the polyanion reduces the molecular weight cut-off of the channels. In the absence of polyanion, VDAC channels allow the passage of inulin and PEG (polyethylene glycol) 3400, but not PEG 8000. After polyanion addition, PEG 1500 does not permeate while gamma cyclodextrin is still able to permeate the VDAC-containing liposomes. It is still unclear whether the polyanion induces VDAC to close, in analogy to a chemical gating process, or simply reduces the channel's permeability. Since this synthetic polyanion acts at very low concentrations, it may mimic a natural substance that gates VDAC in vivo.
Supported by NIH grant GM 28450 and ONR grant N00014-85-K-0651

T-AM-F5 EFFECT OF QUININE ON UNIDIRECTIONAL K^+ FLUX INTO AND OUT OF RESPIRING MITOCHONDRIA. Joyce J. Diwan (Intr. by A. Zelman), Biology Dept., Rensselaer Polytechnic Institute, Troy, NY 12180-3590.

Quinine inhibits some mitochondrial K^+ transport activities, activated by Mg^{++} depletion, swelling, and mersalyl treatment, which have been attributed to a proposed K^+/H^+ exchanger (Nakashima & Garlid, J. Biol. Chem. 257: 9252, 1982; Jung et al., J. Bioenerg. Biomembr. 16: 379, 1984). The present studies examine effects of quinine and related compounds on K^+ flux into and out of isolated rat liver mitochondria respiring on succinate. ^{42}K and atomic absorption were used to monitor unidirectional and net K^+ fluxes. Samples were separated by centrifugation through silicone. 20-28 nmoles quinine per mg protein (100-150 μM) inhibits unidirectional K^+ influx and efflux rates 25 ± 9 (5) and 48 ± 15 (5) percent respectively. [Means of average values from different expts. ± SD (no. of expts)]. As the quinine concentration is increased to 101-112 nmol/mg protein (500 μM) the percent inhibition of K^+ efflux increases to 86 ± 13 (4). The stereoisomer quinidine has similar, but quantitatively smaller inhibitory effects on both K^+ influx and efflux. Quinuclidine, whose protonated ring nitrogen gives quinine a positive charge at physiological pH, when added as a separate compound has no discernable effect on K^+ influx, and at most a small inhibitory effect on K^+ efflux. The greater sensitivity of K^+ efflux to quinine, compared to K^+ influx, is consistent with the proposal that K^+ may enter and leave mitochondria by separate mechanisms. (Supported by NIH Grant GM-20726).

T-AM-F6 THE SPECIFICITY AND THE MECHANISM OF ACTION OF BENZODIAZEPINES AND BENZOTHIAZEPINES ON Na^+-INDUCED Ca^{2+} RELEASE FROM HEART MITOCHONDRIA. M.A. Matlib, Dept. of Pharmacology and Cell Biophysics, University of Cincinnati College of Medicine, Cincinnati, Ohio 45267.

Benzodiazepines and benzothiazepines were found to inhibit Na^+-induced Ca^{2+} release from heart mitochondria in vitro. Among benzodiazepines clonazepam was the most effective, producing a 50% inhibition at 5×10^{-6} M. Among benzothiazepines d-cis-diltiazem was the most effective, producing a 50% inhibition at 7×10^{-6} M. At these concentrations, neither clonazepam nor diltiazem had any effect on Ca^{2+} uptake, respiration, membrane potential, redox state of pyridine nucleotides and light absorbance of mitochondria. The inhibition of Na^+-induced Ca^{2+} release by clonazepam and diltiazem occurred irrespective of species, tissues and assay conditions. No effect of clonazepam or diltiazem was observed on Ca^{2+} release induced by pH, inorganic phosphate, diamide, palmityl-CoA and oxaloacetate. Neither clonazepam nor diltiazem inhibited Na^+/H^+ exchange across the inner membrane. Clonazepam and diltiazem inhibited Na^+-induced Ca^{2+} release without alteration of K_m for Na^+ or intramitochondrial Ca^{2+}. The data indicate that: (1) the inhibitory action of clonazepam and diltiazem on Na^+-induced Ca^{2+} release from heart mitochondria in vitro is direct and specific, (2) the Na^+-induced Ca^{2+} release process is independent of other Ca^{2+} release processes, and (3) the process probably involves a specific Na^+-Ca^{2+} exchange carrier. (Supported by NIH grant HL22619-VA).

T-AM-F7 THE EFFECTS OF MITOCHONDRIAL NADH LEVELS ON RESPIRATION AND THE PHOSPHORYLATION POTENTIAL GENERATED BY ISOLATED MITOCHONDRIA. A.P. Koretsky and R.S.Balaban NHLBI Bethesda MD.

In some previous 31P NMR studies an increase in oxygen consumption (QO2) due to an increase in work was not always accompanied by alterations in the cytosolic phosphorylation potential. This contradicts the prevailing view that ADP, Pi, or ATP levels are the link between an increased work and increased QO2. Therefore we have re-examined the possibility that increases in mitochondrial NADH can stimulate QO2 and/or effect the extra-mitochondrial phosphorylation potential. NADH levels were varied by incubating rat liver mitochondria with various substrates while respiring with added ADP + Pi (State 3) or in a steady state maintained by addition of an ATPase. NADH levels were monitored with a video fluorometer utilizing laser excitation at 340nm and standardized with the 586nm fluorescence from added Rhodamine B. The extra-mitochondrial phosphate potential was monitored by 31P NMR using a chamber which stirred and oxygenated the suspensions in the magnet. The creatine kinase equilibrium was used to quantitate ADP. Increases in mitochondrial NADH with different substrates led to increases in QO2 by mitochondria respiring in State 3. This relationship was linear with a slope of 2.1 (r=.92). Under steady state conditions, the addition of glutamate to mitochondria respiring on pyruvate + malate or citrate alone increased NADH fluorescence and decreased the [ADP] and [Pi] while the QO2 remained constant as driven by the ATPase. Stimulat on of QO2 by added ATPase returned [ADP] and [Pi] to control but at higher than control levels of NADH. These results support the notion that a tissue can increase QO2 by alterations in substrate metabolism, leading to increased NADH levels at a constant phosphorylation state. In this way ATP production can increase in a tissue without sacrificing the free energy of ATP hydrolysis.

T-AM-F8 ON THE REGULATION OF THE H^+-ATPASE IN CHROMATOPHORES OF PHOTOSYNTHETIC BACTERIA. Rita Casadio and B.A.Melandri, Inst.of Botany, Univ.of Bologna, I-4126 Bologna, Italy.

Chromatophores of Rhodobacter sphaeroides, Ga, are endowed with Mg^{2+}-dependent, oligomycin-sensitive ATPase and ATPsynthase activities. The dark-manifest ATPase activity is coupled to the formation of a ΔpH and $\Delta\psi$ with a total sum $\Delta\tilde{\mu}_H+$of 100mV. In the light, $\Delta\tilde{\mu}_H+$sustained by the redox pumps is as high as 380mV and the rate of ATP hydrolysis is two fold stimulated. The dark- and light-ATPase activities are determined as a function of the correspondent $\Delta\tilde{\mu}_H+$progressively decreased under different conditions of uncoupling and inhibition of electron flow. In the dark, the enhancement of the ATPase activity does not correlate univocally with the correspondent decrease of $\Delta\tilde{\mu}_H$and is maximal when in the presence of nigericin, at $\Delta pH=0$,$\Delta\psi$is progressively impaired by adding valinomycin at submicromolar concentrations. In the light, the stimulation of the ATPase activity is affected to a similar degree and in parallel with photophosphorylation by all uncouplers and inhibitors tested. Although the pattern of inhibition of both activities coincides for each set of experimental conditions, no univocal correlation with $\Delta\tilde{\mu}_H+$is observed: impairment of $\Delta\psi$ is more effective than that of ΔpH. $\Delta\psi$,however, is not sufficient to induce light-activation, since high $\Delta\psi$is detected at inhibitory concentrations of antimycin. The relation between both activities and $\Delta\tilde{\mu}_H+$is also different when inhibitors of the b-c_1 redox complex at different sites are utilized. All together these results suggest that the regulation of the ATPase activity is mediated by local interactions within the membrane phase.

T-AM-F9 EVIDENCE FOR CONTROL OF F_1-ATPASE BY LIGAND INDUCED CONFORMATION CHANGE. Jui H. Wang, Bioenergetics Laboratory, Acheson Hall, State University of New York, Buffalo, NY 14214.

The effect of ATP on the fluorescence intensity of bovine heart F_1-ATPase labeled at its essential Lys on β subunit with 7-chloro-4-nitro-2,1,3-benzoxadiazole (N-NBD-F_1) has been examined in 25% glycerol solution containing different concentrations of ADP. In the absence of ADP, the fluorescence of N-NBD-F_1 is unaffected by ATP. But when increasing amounts of ATP are added to a solution of N-NBD-F_1 and 0.37 or 1.0 mM of ADP, the fluorescence intensity of N-NBD-F_1 decreases initially and then increases continually as the concentration of ATP is further raised. The phenomenon can be interpreted in terms of the complementary binding of ATP and ADP and ligand induced conformation change in N-NBD-F_1. Parallel measurements of the suppression of fluorescence of N-NBD-F_1 by medium ADP and the inhibition of the ATPase activity of the unlabeled enzyme by ADP in the preincubation mixture show that there is a quantitative correlation between the two sets of values. The data support the assumption that the ADP which controls the protein conformation is responsible for the observed suppression of ATPase activity. In the ATPase measurements, although the exchange of bound ATP with medium ADP in the Mg^{2+}-free preincubation mixture reached equilibrium in a few minutes, the subsequent back-exchange of bound ADP with medium ATP in the assay mixture was retarded by Mg^{2+}. Consequently, the recorder trace of each assay showed an inhibited rate which was essentially constant over a period of several minutes. But since the enzyme turned over 10^4 times per minute in most of the assays, the responsible ADP had to be bound to auxiliary or regulatory site(s) rather than to another catalytic site which alternates with the first.

T-AM-F10 ELECTROCONFORMATIONAL COUPLING AND FUNCTIONS OF MEMBRANE INTEGRATED PROTEINS.
R. D. Astumian[1], P. B. Chock[1] & T. Y. Tsong[2], [1]Lab. Biochem., Natl. Heart, Lung, & Blood Inst., Bethesda, MD 20205 & [2]Biol. Chem., Johns Hopkins Univ. Sch. of Med., Baltimore, MD 21205.

Many observations indicate that the transmembrane potential, typically between 10-250 mV, can play a critical role in determining the function and activity of membrane bound proteins. Here, we consider the thermodynamic and structural basis for the interaction of an intergral membrane protein with an electric field. It is shown that the influence of an electric field on the conformational equilibrium of a transmembrane protein can be written in the form, $K(E) = K(0)\exp[-(x E^2 + y E)]$, where E is the electric field strength, or simply, the transmembrane potential divided by the membrane thickness; K(E) and K(0) are, respectively, the infield and the zero field equilibrium constants; and x and y are two coefficients charateristic of the protein structure. Structural elements susceptible to electric fields are, net charges, ionizable groups, helices and sheets. Similar equations for individual rate constants of a conformational transition may also be obtained. Changes in the DC electric field can be important in the regulation of membrane protein activity. Additionally, the membrane potential per se can form a reasonable basis for energy transduction when there is a significant oscillatory component. This would be expected in cases where an external AC field is applied to the system, or, in the vicinity of an ion channel where opening and closing of the channel can mediate local polarization and depolarization of the membrane. We have analyzed simple models for such field modulation and examined their properties. (Supported, in part, by NIH Grant GM28795 to T.Y.T.)

T-AM-F11 APPLICATION OF THE ELECTROCONFORMATIONAL COUPLING THEORY TO VOLTAGE INDUCED ACTIVE Rb^+ TRANSPORT AND ATP SYNTHESIS.
T. Y. Tsong[1], R. D. Astumian[2] & P. B. Chock[2], [1]Biol. Chem., Johns Hopkins Sch. of Med., Baltimore, MD 21205, & [2]Natl. Heart, Lung, & Blood Inst., Bethesda, MD 20205

Protein molecules are structurally competent for absorbing free energy from an oscillating electric field and using it to do chemical or transport work. Membrane-bound enzymes are likely to perform this task because they experience a field strength of 20-500 kV/cm (10-250 mV transmembrane potential) (Tsong & Astumian, Bioelectrochem. Bioenerg. In press; see also the preceding abstract). Here we present a kinetic model that is capable of transducing free energy from an oscillating electric field. The model consists of substrate binding and product release steps linked through two electroconformational coupling steps which mediate energy absorption and conversion. When applied to transport ATPases, these four steps correspond to steps for enzyme activation, ligand binding, ligand translocation, and ligand release. Computer simulations reproduced the frequency and field strength characteristics of voltage induced Rb^+ and K^+ transport by (Na,K)ATPase of human erythrocytes. Extension to the case of ATP synthesis induced by pulsed electric fields leads to the suggestion that the F_0F_1 ATP synthetase is capable of internally modulating a DC transmembrane potential by the opening and closing of the F_0 channel. In these experiments, it was found that up to 8-12 ATPs per enzyme were synthesized by a single 100 microsecond electric pulse. This very high rate of synthesis can be explained by the field dependence of the rate constants for the reaction steps. (Supported by NIH Grant GM28795 to T.Y.T.)

T-AM-G1 HALORHODOPSIN IS NOT A HOMOGENEOUS SPECTRAL SPECIES IN THE NATIVE ENVIRONMENT. D.B.Bivin and R.A. Bogomolni, Cardiovasc. Res. Inst. and Dept. Biochemistry and Biophysics, University of California, San Francisco, CA 94143.

Light-adapted, detergent-free, purified halorhodopsin absorbs maximally at around 578nm, hR_{578}, at 25°C, pH 7 in 4M NaCl. Because this form is the one generated in the dark by addition of all-trans retinal to the apoprotein it is presumably a homogeneous species. Upon illumination, for 30-60 seconds with red light ($\lambda \geq 600$nm), hR_{578} shifts to shorter wavelength generating hR^{RA} (RA = red light-adapted), a thermally stable species. Photoexcitation of hR^{RA} generates, with low quantum efficiency ($\phi \leq 0.01$), a thermally metastable form that absorbs maximally around 408nm (hR_{408}) with release of a proton to the medium. The thermal decay half-time is ~ 500sec at 20°C. The difference spectra for both the photo (forward) or thermal (back) conversion shows a single isosbestic point at ~450nm and characteristic maxima and minima (or vice versa) at 408nm and 555nm (apparently the absorption maximum of hR^{RA}) respectively. Because irradiation at 530nm (where hR_{408} absorption is negligible) fully restores the original 578nm absorbance we conclude that hR^{RA} photoconverts to hR_{578}. The relative species concentration in this photochromic system is therefore determined by the color and intensity of irradiation. These photo and thermal reactions have been observed, with small variations in kinetics, in the purified pigment, in isolated membranes, in sonicated envelope vesicles and in intact cells. Action spectroscopy strongly suggests that hR_{578} is the active light-driven anion pump. The physiological role of hR^{RA} and hR_{408} is not yet understood, but it is speculated that they may be involved in the regulation of pump activity.
This work was supported by NIH grant GM-27057.

T-AM-G2 HALORHODOPSIN PHOTOCYCLE STUDIES. Aihua Xie[1], Richard H. Lozier[2], and Roberto A. Bogomolni[2]. [1]Department of Physics, Carnegie-Mellon University, Pittsburgh, PA 15213, and [2]Departments of Biochemistry and Biophysics, and Cardiovascular Research Institute, University of California, San Francisco, CA 94143.

Halorhodopsins (hR) were purified using detergents as described by Taylor, Bogomolni and Weber (Proc. Natl. Acad. Sci. 80, 6172-76 (1983)). The detergents were removed from hR by dialysis against 30 mM HEPES buffer at 3 M NaCl and pH 7. The hR sample was then adjusted to pH 7, and optical density 0.55. The photocycle of hR, which has absorption maximum at 578nm, was probed using flash spectroscopy. The flash induced absorption changes of hR were measured at seven temperatures and multiple wavelengths: at 460nm, 560nm, 640nm and 680nm at 5°C, 15°C, 25°C and 35°C, and at fourteen wavelengths from 440nm to 700nm, at 10°C, 20°C and 30°C; and in wide time windows, from 1 μs to 300 ms. The data analysis employs the methods developed for photocycle kinetics studies of bacteriorhodopsins (Nagle et al, Biophys. J. 38, 161 (1982)) with recent extensions to include distributed kinetics. The simple kinetics analysis requires four intermediates, while a distributed kinetics analysis, assuming that the last decay is distributed, requires three intermediates. Several kinetic models were analyzed, such as unidirectional, unbranched models; backreaction models; and branched models. Compared to previous reports by other investigators, no red shift intermediate is found in the late photocycle of hR. This work was supported in part by NIH grant GM-27057.

T-AM-G3 EVIDENCE FOR DISTRIBUTED BARRIER HEIGHTS IN BACTERIORHODOPSIN. **G.W. Rayfield, Physics Department, University of Oregon, Eugene, OR 97403**

It is shown that the inclusion of a distribution of activation energies about some mean value significantly improves the fit of a photoresponse curve of bacteriorhodopsin to a sum of exponentials. A gaussian distribution of activation energies is assumed. Only two exponential components are required to fit the photoresponse from 1 μs to 1 second. The time course of a particular exponential component in the photoresponse is given by:

$$(1)\quad V_i(t) = A_i \int g_i(E)\,(1-\exp(-\lambda_i(E)t))\,dE$$

$$(2)\quad \lambda_i(E) = C_i \exp(-E/kT)$$

where g_i is the probability of having an activation energy between E and E+dE. All of the constants necessary for the fit are derived from a photovoltage versus log time plot except for σ. Numerical integration is used to evaluate the integrals. This concept of distributed kinetics has already been successfully applied to other biological problems (1,2). **This work was supported by NIH grant GM 26669.**

references:

1. Austin, R. H., Beeson, K., Eisenstein, L., Frauenfelder, H., Gunsalus, I. C. and Marshall, V. P. 1974. Phys. Rev. Lett. 32:403-405.

2. Xie, A. H., Nagle, J.F. and Lozier, R. H. 1985. Biophys. J. 47:98a.

T-AM-G4 RETINAL PROTEIN INTERACTIONS IN BACTERIORHODOPSIN AND BACTERIAL SENSORY RHODOPSIN
Hillary Rodman[a] & Barry Honig[a], Koji Nakanishi[b], Masami Okabe[b] & Nobuko Shimizu[b], John L. Spudich[c] & Donald A. McCain[c], [a]Dept. of Biochemistry & Molecular Biophysics, Columbia University, New York, NY 10032, [b]Dept. of Chemistry, Columbia University, New York, NY 10027, [c]Dept. of Anatomy and Structural Biology, Albert Einstein College of Medicine, Bronx, NY 10461

Retinal analogs with altered conjugated double bond systems have provided a versatile tool in detecting spectroscopic determinants in retinal based pigments. Several years ago, the application of this technique to BR led to the suggestion that a negatively charged amino acid interacting with the ring terminus of the chromophore was responsible for producing the absorption maximum of this pigment. It was assumed at the time that a positively charged group which formed an ion pair with the negative charge interacted only weakly with retinal. A number of new observations require a significant modification of this model. These include a correction of an erroneous absorption maximum reported previously, new data on retinal analogs with altered ring stereochemistry and NMR evidence of a planar s-trans ring-chain conformation. Theoretical calculations of absorption maxima indicate that the available body of data can best be fit by a model in which both members of the ion pair interact with the chromophore and produce an approximately 1500 cm^{-1} opsin shift". The remaining 3500 cm^{-1} of the opsin shift in BR appear due to a perturbation near the Schiff base, possibly a weakened counterion interaction, and to the planar ring chain conformation. The evidence that suggests these conclusions and the details of the new model will be discussed. Related experiments on SR demonstrate that the same overall electrostatic and steric properties of the retinal binding site exist in both proteins despite their different functions.

T-AM-G5 LOCATION OF CHEMICALLY MODIFIED LYSINE 41 IN THE STRUCTURE OF BACTERIORHODOPSIN BY NEUTRON DIFFRACTION. F. Seiff, I. Wallat, J. Westerhausen and M.P. Heyn, Biophysics Group, Freie Universität Berlin, Berlin, FRG.

Purple membranes were prepared in which bacteriorhodopsin was labelled at lysine 41 with phenylisothiocyanate (PITC) and with perdeuterated PITC. The in-plane position of this small label containing only five deuterons was determined from the differences between the neutron diffraction intensities of the two samples. At 8.7 Å resolution the Fourier difference map revealed a well-defined site between helices 3 and 4. This position was confirmed by a refinement procedure in reciprocal space. Model calculations showed that the observed difference density had the right amplitude for the label. It is thus possible to locate a small group in a large protein structure by replacing as few as five hydrogens by deuterium. The observed location of PITC restricts the number of possibilities for the assignment of helix B in the sequence (to which lysine 41 is attached) to one of the seven helices of the structure. Taking into account the size of the label and the length of the lysine side chain our result excludes helices 1, 2 and 7 as candidates for B.

T-AM-G6 RETINAL ANALOGUES SHOW THAT THE OPSIN SHIFT IN BACTERIORHODOPSIN IS DUE TO A 6-S-TRANS RETINAL CHROMOPHORE WITH A PERTURBED SCHIFF BASE. J. Lugtenburg, M. Muradin-Szweykowska, R. van der Steen, C. Heeremans, Dept. of Chemistry, Leiden University, The Netherlands; G.S. Harbison and J. Herzfeld, Harvard Medical School, Boston, MA; R.G. Griffin, MIT, Cambridge, MA; S.O. Smith and R.A. Mathies, Dept. of Chemistry, Univ. of Calif., Berkeley, CA

The mechanism of the "opsin shift" in bacteriorhodopsin (BR) has been studied with dihydro retinal derivatives and with analogues whose C_6-C_7 conformation is covalently locked. We find the bacterioopsin shifts for the 5,6- and 7,8-dihydro derivatives to be 2300 and 3500 cm^{-1}, respectively. The large residual opsin shift for 7,8-dihydro BR (385→445 nm) indicates that ~70% of the opsin shift arises from chromophore-protein interactions near the Schiff base. Analogues with the β-ionone ring locked in the 6-s-trans or in the 6-s-cis conformation were also studied. The locked 6-s-trans analogue binds rapidly to bacteriorhodopsin, shows light-dark adaptation, and has 90% proton pump activity. Its λ_{max} (564 nm) is close to that of the native chromophore and the opsin shift is 3800 cm^{-1}. The nearly native behavior of the locked 6-s-trans analogue provides strong additional evidence that bacterio-opsin selectively binds the 6-s-trans conformer. 6-s-Trans isomerization is shown to produce a 1200 cm^{-1} red shift in model protonated retinal Schiff bases. This effect, together with the 3500-3800 cm^{-1} opsin shift caused by Schiff base perturbation, accounts for nearly all of the 5100 cm^{-1} opsin shift observed in BR. These results strongly support previous CP-MASS ^{13}C and ^{15}N NMR studies, which indicate that the chromophore in BR is in the 6-s-trans conformation, interacts with a dipolar pair of opsin charges near C_5...C_7, and has a weakly hydrogen-bonded Schiff base nitrogen.

T-AM-G7 STRUCTURAL CHANGES INVOLVED IN PURPLE TO BLUE TRANSITION OF PURPLE MEMBRANES, Nandini Katre*, University of California, San Francisco, CA

Using X-ray diffraction techniques, the structural changes involved in the reversible purple to blue transition of membranes containing bacteriorhodopsin has been studied. This purple to blue transition can be generated by removal of bound cations from purple membranes [Kimura, et al. (1984) Photochem. Photobiol. 40, 641-646 and Chang et al. (1985) PNAS 82, 396-400]. The proteolytic cleavage of the C-terminal peptide of bacteriorhodopsin also causes the purple → blue transition. X-ray diffraction patterns were obtained from blue membranes, papain cleaved membranes and blue membranes titrated with heavy metal cations (Pb^{2+}). Fourier difference maps showed that the purple to blue transition in the bR membranes did not cause major structural changes. The cations titrated back to revert the membranes from blue to purple can be located on the projected structure of bacteriorhodopsin. Recent studies (Dupuis et al. (1985) PNAS, 82, 3662-3664) have suggested a functional role for these bound cations on PM. This work was done in Robert M. Stroud's laboratory in the Dept. of Biochem. and Biophysics at University of California, San Francisco, CA.

* Present address: Cetus Corporation, 1400 Fifty-Third St., Emeryville, CA 94608.

T-AM-G8 THE CATION-INDUCED BLUE TO PURPLE TRANSITION IN BACTERIORHODOPSIN. M.K. Mathew, P. Scherrer, W. Sperling, and W. Stoeckenius; Cardiovascular Research Institute and Dept. of Biochemistry and Biophysics, University of California, San Francisco, Ca 94143-0130.

Deionized bacteriorhodopsin (bR) absorbs maximally at ~605nm, appears blue, and can be reconstituted to purple membrane with cations. The retinylidene chromophore in blue membrane is almost equally divided between 13-cis and all-trans conformers in the dark-adapted state as estimated by extraction and subsequent HPLC analysis of the aldehydes. In the light-adapted pigment at least 2/3 of the chromophores are in the all-trans form. Dark adaptation is rapid with a half-time of less than 30 seconds. Addition of cations in substoichiometric amounts to the dark-adapted membrane shifts the absorption maximum of a fraction of the bR molecules to ~568nm in less than 5 seconds with only a small change in the isomer ratio. This species also undergoes light adaptation to almost completely all-trans with a λ_{max} at ~575nm and dark-adapts again to λ_{max} ~568nm. Thus it is clearly not equivalent to native purple membrane. Stopped flow analysis of the reconstitution process revealed at least two steps, the faster one with a halftime of ~10ms. Partially reconstituted membranes dark-adapt rapidly ($T_{1/2}$ ~90sec for 1:0.5 bR/Mn^{++}, pH 7.0) We conclude that there is at least one intermediate form of bacteriorhodopsin in the cation-induced blue to purple transition.

T-AM-G9 DIAMINONAPHTHALENE RETINAL COMPLEXES: A UNIQUE MODEL SYSTEM FOR INVESTIGATING CONTROLLED PROTONATION AND LONE PAIR ELECTRON INTERACTIONS WITH RETINYLIDENE SCHIFF BASES.
J. Y. Huang*, A. Lewis*, Y. N. Shie**, J. MacMurray**. Depts. of Applied Physics* and Chemistry**, Cornell University, Ithaca, N.Y. 14853

A diaminonaphthalene compound has been synthesized that allows selective reaction of retinaldehydes. The resulting Schiff base complexes of this compound allow us to delineate the effect of an amino group in close and fixed proximity to the Schiff base. For the unprotonated Schiff base complex, we have detected significant alterations in both the absorption and resonance Raman spectra due to the presence of a second amino group 2.4Å from the Schiff base. An absorption band at 396 nm was observed, which shifts to 368 nm when the second amino group is present. The presence of the amino group also induces an increase in frequency of the retinylidene chromophore c=c stretching vibration from 1560 cm^{-1} to 1567 cm^{-1}. In the protonated complex, a similar but larger absorption blue shift is detected in going from the monoamino (504 nm) to the diamino species (450 nm). The resonance Raman spectra of these molecules show a shift in the c=c stretching frequency from 1567 cm^{-1} (unprotonated) to 1555 cm^{-1} (protonated) while the C-H bend frequency upshifts from 963 cm^{-1} to 972 cm^{-1} in a manner that is similar to what is observed in going from the bR_{570} to the M_{412} species in bacteriorhodopsin. Our findings indicate that the protonated diaminonaphthalene retinylidene chromophore achieves a molecular structure in which the Schiff base proton is shared equally by the two amino groups. Such diaminonaphthalene complexes allow us to monitor the effect of controlled protonation of the Schiff base on the spectral properties of retinylidene chromophores.

T-AM-G10 RETINAL IN THE PURPLE MEMBRANE IS INACCESSIBLE TO BOTH NEUTRAL AND NEGATIVE TERBIUM CHELATES BY DIFFUSION-ENHANCED ENERGY TRANSFER. Richard O. Leder and David D. Thomas, Department of Biochemistry, University of Minnesota Medical School, Minneapolis, MN 55455.

Although the structure of bacteriorhodopsin (BR) has been refined to <5 Å, the position of retinal relative to either surface of the native purple membrane remains poorly resolved. We have measured the distance of closest approach between aqueous chelates of terbium (Tb) and the chromophore of BR using diffusion-enhanced energy transfer in the rapid-diffusion limit.

We have reported previously that the transition moment of retinylidene-lysine lies within 10 Å of a negatively-charged surface of the purple membrane (Thomas and Stryer, Fed.Proc.39(1980): 1847). Energy transfer from Tb chelates to light-adapted purple membrane sheets is now shown to be: (a)inconsistent with chelate-retinal contact; and (b) asymmetric with respect the membrane surfaces (Henderson,J.Mol.Biol.93(1975):123) assuming a membrane thickness of 51.7 angstroms.

Donor		TbHED3A [0]	TbEDTA [-1]	Tb(DPA) [-3]
Closest-approach distance (Å)	10mM/2M	14.4/14.9	31.3/18.2	38.0/20.0
Approximate chelate radius (Å)		4.0	4.0	6.4
Effective retinal depth (Å)	10mM/2M	10.4/10.9	27.3/14.2	31.6/13.6

Transfer rates increase with increasing ionic strength only for negative chelates. This salt dependence does not saturate even at 1M NaCl, but for each donor, the closest-approach distance tends toward that of the neutral probe. We will address the possibility that simple membrane screening effects are enhanced by local effects of salts on BR. We thank W.Sperling, S.L. Helgerson and M.K.Mathew for invaluable assistance.

T-AM-G11 MECHANISM OF DIVALENT CATION BINDING BY BACTERIORHODOPSIN -- C. -H. CHANG, R. JONAS, S. MELCHIORE, R. GOVINDJEE, T.G. EBREY. DEPARTMENT OF PHYSIOLOGY AND BIOPHYSICS, UNIVERSITY OF ILLINOIS, URBANA, ILLINOIS 61801.

Several observations have already suggested that the carboxyl groups are involved in the association of divalent cations with bacteriorhodopsin (Chang et al., 1985). Here we show that at least part of the protons release from deionized purple membrane (blue membrane) samples when salt is added are from carboxyl groups. We find that the apparent pK of magnesium binding to purple membrane in the presence of 0.5 mM buffer is 5.85 which is shifted from that of the carboxyl groups, 4.0 - 4.4. This shift in the pK is attributed to the proton concentrating effect of the large negative surface potential of the purple membrane.

Divalent cations may interact with negatively charged sites on the surface of purple membrane through the surface potential and/or through conformation dependent chelation. We find that divalent cations can be released from purple membrane by raising the temperature. Moreover, purple membrane loses some capacity to bind divalent cations after bleaching. Neither of these operations should decrease the surface potential and thus they suggest that some specific conformation in purple membrane is essential for the binding of a substantial fraction of the divalent cations.

T-AM-G12 CATION BINDING CHANGES DURING THE BACTERIORHODOPSIN PHOTOCYCLE. R.A. Bogomolni, W. Hubbell, and W. Stoeckenius. Dept. of Biochemistry and Biophysics, and CVRI, University of California, San Francisco, CA 94143; and Jules Stein Eye Institute, University of California School of Medicine, Los Angeles, CA 90024.

Electron Paramagnetic Resonance (epr) was used to monitor binding changes of paramagnetic cations during the photocycle of bacteriorhodopsin (bR). Aqueous suspensions of purple membrane were regenerated from deionized (blue) membranes by addition of Mn^{++} or a cationic phosphonium nitroxide spin label. In the concentration range used (cation/bR = 1:1 to 5:1) these cations showed epr spectra characteristic of mixtures of free and partially immobilized, "bound" populations. The latter fraction increased with increasing pH in the range tested (3.8-8.0). Excitation of the sample with xenon strobe flashes (1msec, 530-700nm) caused a transient increase in the concentration of free cation at acidic pH (3.8-5.0). At higher pH (6.5-8), however, the signal reversed sign, indicating transient cation uptake. We also measured the light-induced changes in pH of these samples using a fast-response glass electrode (~2msec). We observed transient proton uptake at acidic pH (3.8-5.5) which reverses to proton release at higher pH (6.5-8). The observed cation binding changes are consistent with the expected changes in surface potential resulting from the changes in protonation of surface groups during the bR photocycle. They occur, presumably, at opposite sides of the membrane, in opposite direction, and with different pK's but overlap in time. For this reason the stoichiometry of the cation exchanges has not yet been resolved. This work was supported by NIH grant GM-27057(R.A.B., W.S.); and by the Jules Stein Professorship Endowment and NIH grant EY-05216(W.H.).